Mohamed Khider University of Biskra
Faculty of exact sciences and natural and life sciences
Materialsciences department

MASTER MEMORY

Domain of Matter Sciences

Section of Physics

Speciality of Materials Physics

Réf. :

Prsented by:
Brahimi Lakhdar

The: 13/6/2023

The effect of bromine doping rate on the properties of ZnO thin films

---

Jury:

Mr.	ATTAF Abdallah	Professor	University of Biskra	Presidant
Mrs.	Hamani Nadjette	MCB	University of Biskra	Supervisor
Mrs.	Bennaceur Kheira	MCB	University of Biskra	Examiner

Academic Year: 2022\2023

Acknowledgments

First, we thank Almighty Allah who enabled my to do this work. We thank Him, Glory be to Him, for bestowing upon by the grace of completeness. Next, I would like to express my love, respect and appreciation to my family for their unconditional support, understanding and dedication throughout these years. I also thank very much to my director, Dr. ***Hamani Nadjette****, for her patience and continuous follow-up throughout the realization of this anniversary.I also thank warmly the members of the jury: Professor* ***Attaf Abdallah*** *and Dr.* ***Bennaceur Kheira****, for their approval to review my work.*

DEDICATION

I dedicate this Work

To my mother who supported me

to make this Work easier

To all my family

And my friends

List of contents

.

Chapter II: Spray pyrolysis and characterization methods

Chapter III: Results and discussions

LIST OF FIGURES

LIST OF TABLES

General Introduction

Transparent and conductive oxides (TCO) are remarkable materials in many areas. The existence of their double property, electrical conductivity and transparency in the visible, makes them ideal candidates for optoelectronics, photovoltaic or electrochromic windows.

TCOs are binary or tertiary metal oxides with high free carrier density, outstanding electrical conductivity, and high optical transmittance in the UV-VIS-NIR band. Because intrinsic, stoichiometric TCOs lack high conductivity and transmittance, these properties can be acquired by employing suitable dopants, resulting in oxides with a non-stoichiometric composition. Zinc oxide, one of these transparent semiconductor oxides, has excellent electrical and optical properties; its optical energy gap (3.37ev) makes it a suitable product [1]. Suitable for optoelectronic applications such as the fabrication of transparent electrodes [2]. UV detectors, or laser diodes generating blue light [3]. Many processes may be used to generate zinc oxide as a thin film, including spray pyrolysis, sputtering, sol-gel, pulsed laser deposition (PLD), and chemical vapor deposition (CVD) Spray pyrolysis is regarded as a low-cost and effective technique among them [4].

Many techniques have been employed to characterize the films and hence identify optimum growth conditions (for example, X-ray diffraction, electron microscopy, ultraviolet-visible spectroscopy and Four-point probe).

In this context, we chose zinc oxide as the basic material. Indeed, it is an available materiel and easy to deposit as thin films. The aim of this work was to prepare undoped and bromine doped ZnO thin films by pneumatic spray pyrolysis, in order to obtain a high thin film quality.

This work is divided into three chapters. In the first chapter, we make a brief summary of the physical properties (optical, electrical...) of zinc oxide (ZnO) material with its applications. Then, we explain various depositions techniques used to deposit ZnO films.

In the second chapter, we bring detail information about Spray pyrolysis. In addition, we explain the methods which are used in this work for the characterization of the ZnO films (like structural, optical, and electrical measurements).

The last chapter presents the characterization results of Zinc oxide thin films doped with different concentration of Bromine; where the aim is for finding out the effect of doping rate on the ZnO characteristics; the films were synthesized by pneumatic spray pyrolysis technique; in line with this the results have get enough interpretation and discussion.

Finally we will conclude our work by a general conclusion including details results of characterization of zinc oxide thin films.

References

[1] Jagadish, C., &Pearton, S. J. (Eds.). Zinc oxide bulk, thin films and nanostructures: processing, properties, and applications. Elsevier. (2011).

[2] Idris, M. M., Olarinoye, I. O., Kolo, M. T., & Ibrahim, S. O. Transparent conducting oxides thin film dosimetry: Present and the future. (2022).

[3] Babar, A. R., Shinde, S. S., Moholkar, A. V., Bhosale, C. H., & Rajpure, K. Y. Structural and optoelectronic properties of sprayed Sb: SnO2 thin films: Effects of substrate temperature and nozzle-to-substrate distance. Journal of Semiconductors, 32(10), 102001. (2011).

[4] Othmane, M. Synthesis and characterization of Zinc Oxide (ZnO) Thin films deposited by spray pyrolysis for applying: electronics and photonics (Doctoral dissertation, University Mohamed Khider of Biskra).(2018).

Chapter I:

Bibliographic studies of zinc oxide

In this chapter we will summarize the fundamental physical properties of zinc oxide (ZnO) thin film and their applications. Then, the depositions techniques that are used to develop SnO_2 thin films and which are going to be described later on.

I.1 Transparent conductive oxides

Transparent conducting oxides (TCOs), like SnO_2, In_2O_3 and ZnO, have a wide range of applications in optoelectronic devices, owing to their unique combination of high electrical conductivity and optical transparency in the visible spectrum of light. The development of TCO coatings seems to be an important application of thin film technology, which works as window layers transparent to solar radiation and electrical contacts [1].

Transparent conducting oxides (TCO) constitutes of a specific group of materials that contain high transparent and conductivity. TCOs come from different materials. In addition, they are typically normal semiconductors, doped with one or more sorts of impurities. The dopants and native defects have important role in these systems which are to control the conductivity. As a result, defects take part to conductivity in a semiconductor, which is optically transparent. A desired TCO material would have more than 80% optical transmission in the visible light range, a carrier concentration of the order of 10^{20} cm^{-3} and a resistivity of the order of 10^{-3} Ω cm. [2]

I.2 Zinc oxide

Zinc Oxide is a semiconductor. It exists in natural form, under the name of "Zincite", but can also be synthesized artificially in solid form "ZnO bulk" with different colors depending to the impurities that it contains [3].

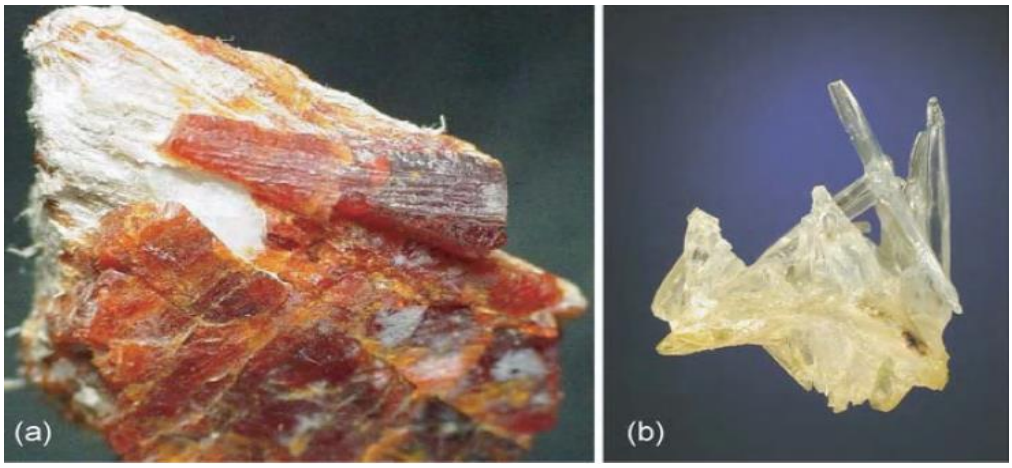

Fig.I.1. ZnO bulk in natural form (a) and from hydrothermal synthesis (b) [4].

I.3 properties of ZnO

I.3.1 The crystallographic properties:

ZnO is an II-VI compound semiconductor with wurtzite, zinc blend, and rocksalt crystal structures .Fig I.2 depicts these structures [4]

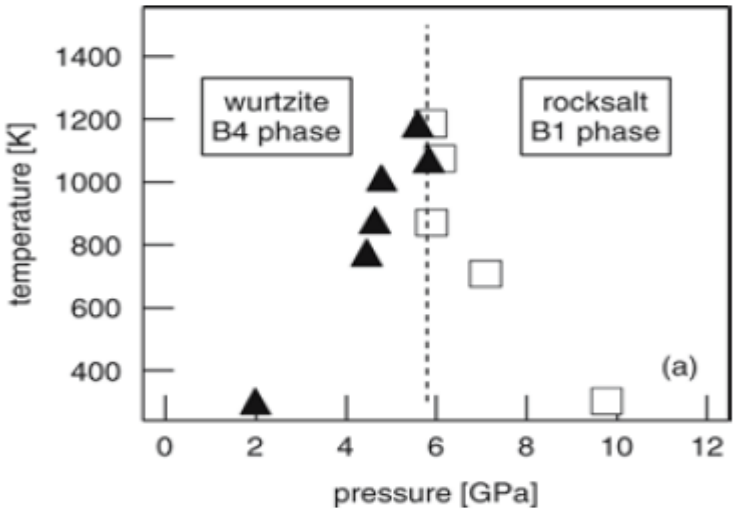

Fig.1.2. Phase diagram of ZnO.

Zinc oxide crystallizes in three forms: hexagonal wurtzite, cubic zinc blende, and the rarely observed cubic rocksalt. The wurtzite structure is most stable and thus most common at ambient conditions. The zinc blende form can be stabilized by growing ZnO on substrates with cubic lattice structure. In both cases, the zinc and oxide are tetrahedral. The rocksalt NaCl-type structure is only observed at relatively high pressures ~10 GPa [5]

The hexagonal and zinc blende ZnO lattices have no inversion symmetry (reflection of a crystal relatively any given point does not transform it into itself). This and other lattice symmetry properties result in piezoelectricity of the hexagonal and zinc blende ZnO, and in pyro-electricity of hexagonal ZnO [5].

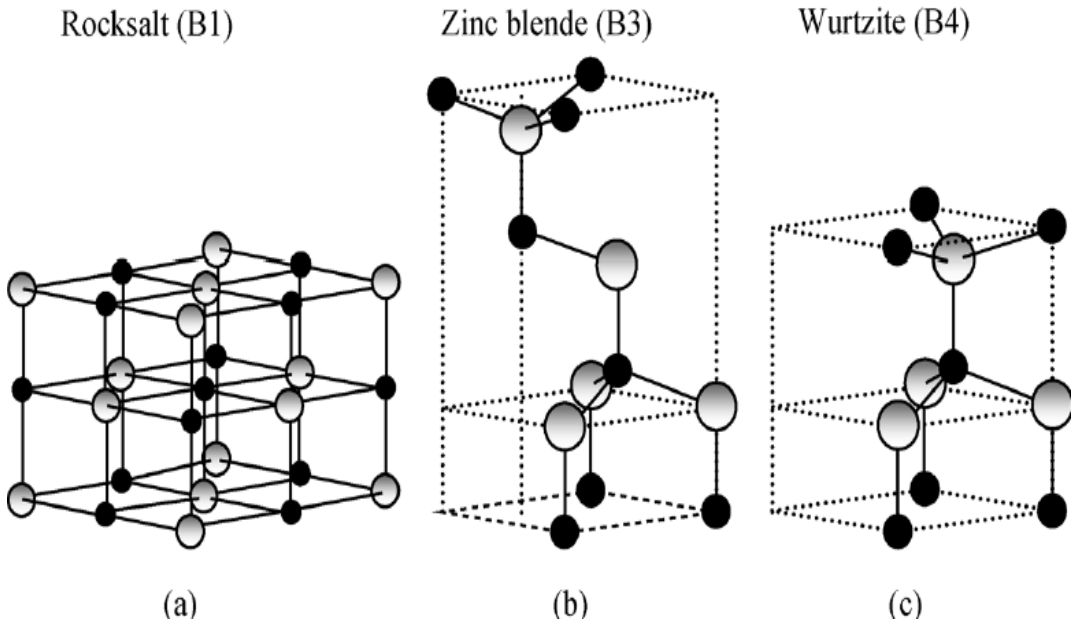

Fig I.3. Crystal structures of ZnO (a) rock salt (b) zinc blend and (c) wurtzite hexagonal.

The wurtzite crystal structure is the most stable structure of ZnO and it has also been found theoretically that this crystal structure is energetically favorable compared to the rocksalt and zinc blend structure. [6]. Fig I.4 depicts these structures from various angles.

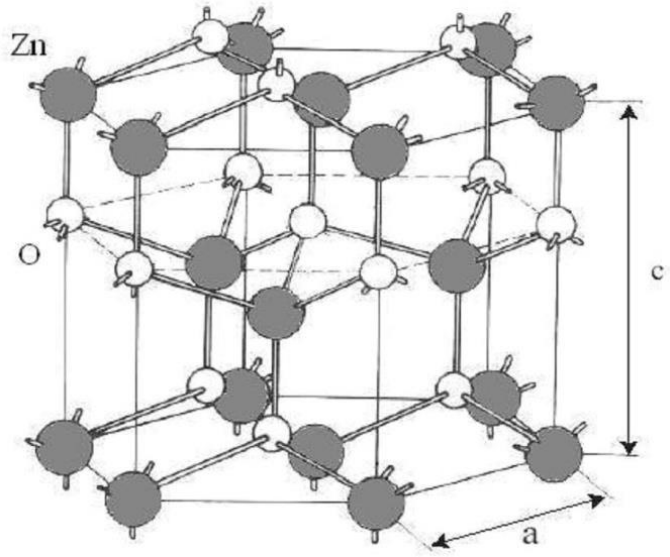

Fig I.4.The schematic diagram of the wurtzite crystal structure of ZnO

The wurtzite structure consists of a hexagonal unit cell with two lattice parameters a and c with (a = 0.3296 and c = 0.520 65 nm [7]) in the ratio of $\frac{c}{a}=\sqrt{8/3}$ =1.633 (in an ideal wurtzite structure) . It is characterized by two interconnecting sub lattices of Zn^{+2} and O^{-2}, such

that each Zn ion is surrounded by tetrahedral of O ions, and vice-versa. This tetrahedral coordination gives rise to polar symmetry along the hexagonal axis. Various physical properties of the hexagonal structure of zinc oxide are summarized in Tab I.1. [7]

Table I.1: Physical properties of the zinc oxide in the wurtzite [8]

Properties	Properties parameters (Value) at 300 K
Crystalline structure	Wurtzite
Lattice parameters	$a_0 = b_0 = 3.249$ Å $c_0 = 5.206$ Å
Refractive index	2. 008 – 2.029
Band gap energy	3.37 eV, direct
Melting point	1975°C
Density (g/cm^3)	5.606
Exciton binding energy	60 meV
Electron effective mass	0.28 m_0
Bandgap	3.4eV(direct band gap)

I.3.2. Electronic Structure of ZnO

ZnO is a direct band gap material. Fig I.5 depicts the band structure of ZnO. It can be seen that in the Brillion zone at k = 0, the lowest of the conduction band and the highest of the valence band are located at the same point. Zn has the electron configuration 1s2 2s2 2p6 3s2 3p6 and O has the electron configuration 1s2 2s2 3p4. The bottom of the conduction band in a ZnO crystal is caused by occupied 2p states of O^{2-}, and the top of the valence band is caused by empty 4s states of Zn^{2+}. Under the influence of spin, the valence band further divides into three sub valence bands, as illustrated in Fig I.5 [9]

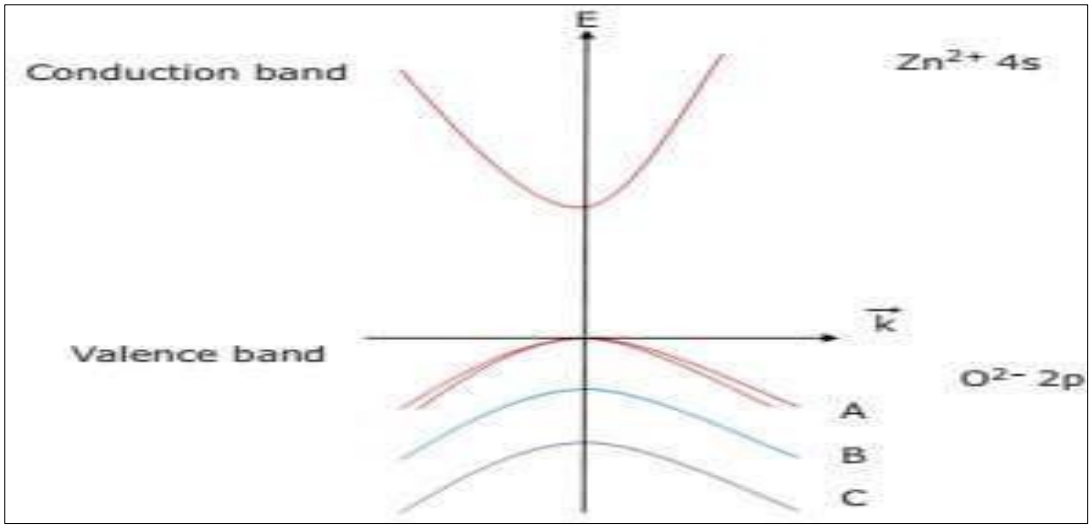

Fig I.5 Electronic band structure of ZnO [9]

I.3.3 Electrical properties:

ZnO has a relatively large direct band gap of ~3.3 eV at room temperature; therefore, pure ZnO is colorless and transparent. Advantages associated with a large band gap include higher breakdown voltages, ability to sustain large electric fields, lower electronic noise, and high temperature and high-power operation. The bandgap of ZnO can further be tuned from ~3 – 4 eV by its alloying with magnesium oxide or cadmium oxide.

Most Zinc oxide has *n*-type character, even in the absence of intended doping. Native defects such as oxygen vacancies or zinc interstitials are often assumed to be the origin of this, an alternative explanation has been proposed, based on theoretical calculations, that unintentional substitution hydrogen impurities are responsible. Controllable n-type doping is easily achieved by substituting Zn with group-III elements Al, Ga, In; then, according to the majority of reports in ZnO films deposited using various methods, resistivity and mobility were nearly independent of the deposition method and were limited to about 2×10^{-4} cm and 50 cm^2/Vs, respectively . Furthermore, it is difficult to be certain about ZnO in p-type; this problem stems from the limited solubility of p-type dopants and their compensation by numerous n-type impurities, and it applies not only to ZnO but also to related compounds GaN and ZnSe. Measurement of p-type in "intrinsically" n-type material is similarly difficult due to inhomogeneity, which produces misleading signals. However, such high levels of p-conductivity are dubious and have yet to be experimentally validated [10].

I.4. Doping of ZnO:

Many types of dopants have been used (Al , In , As , S , Sn , Mn ,Br,.. etc.) for many important applications in ZnO thin films; these dopant elements offer a manner to regulate the electrical, optical, and magnetic properties, which are make doped ZnO films are promising candidates as conductors with high transparency in the visible light range and high conductivity. Even though the standard transparent conductors in industry are ITO and FTO, there is huge interest in finding more stable and cheaper alternatives [10].

In Table 1.2 some doped films are summarized, and their transmittance in the visible range, and lowest resistivity values too, There are a Typical dopants that have been used to increase the conductivity of ZnO are group III (B, Al, In, Ga) and group IV (Pb, Sn) elements of the periodic table

Table I.2 Summary of different doped ZnO thin films as transparent conductors. [10].

Dopant	Methods	Transmitance in visible range	Lowest resistivity
Al	Pulsed laser deposition (PLD)	~90%	$\sim 10^{-4}$ Ωcm
	Radio-frequency (RF) magnetron sputtering		
	Solution processed		
Ga	PLD	~85%	$\sim 10^{-3}$Ωcm
	Solution processed		
In	Solution processed	~80%	~20 Ωcm
N	Plasma-assisted molecular beam epitaxy	~80%	$\sim 10^{-2}$ Ωcm
	RF magnetron sputtering		
	Solution processed		

I.5. Applications of Zinc Oxide:

Zinc oxide is widely used in variety of applications due to its diverse chemical and physical properties. It is used in a wide variety of applications, ranging from treys to ceramics, pharmaceuticals to agriculture, and paints to chemicals.

The Major applications of zinc oxide thin films are in the rubber industry. ZnO along with stearic acid is used in the vulcanization of rubber to produce such things as tires, shoe soles, and even hockey pucks.

A very important use is that Zinc Oxide is widely used as the buffer layer in CIGS (Copper Indium Gallium Selenide) solar cells. Some current experiments are focusing on the effect of the thickness of ZnO on maximum power output for the cells.

Zinc Oxide also has antibacterial and deodorizing properties. For this reason it is employed in medical applications such as in baby powder and creams to treat conditions such as diaper rash, other skin irritations and even dandruff. Due to its reflective properties it is also used in sun blocks and can often be seen on the nose and lips of lifeguards at the beach

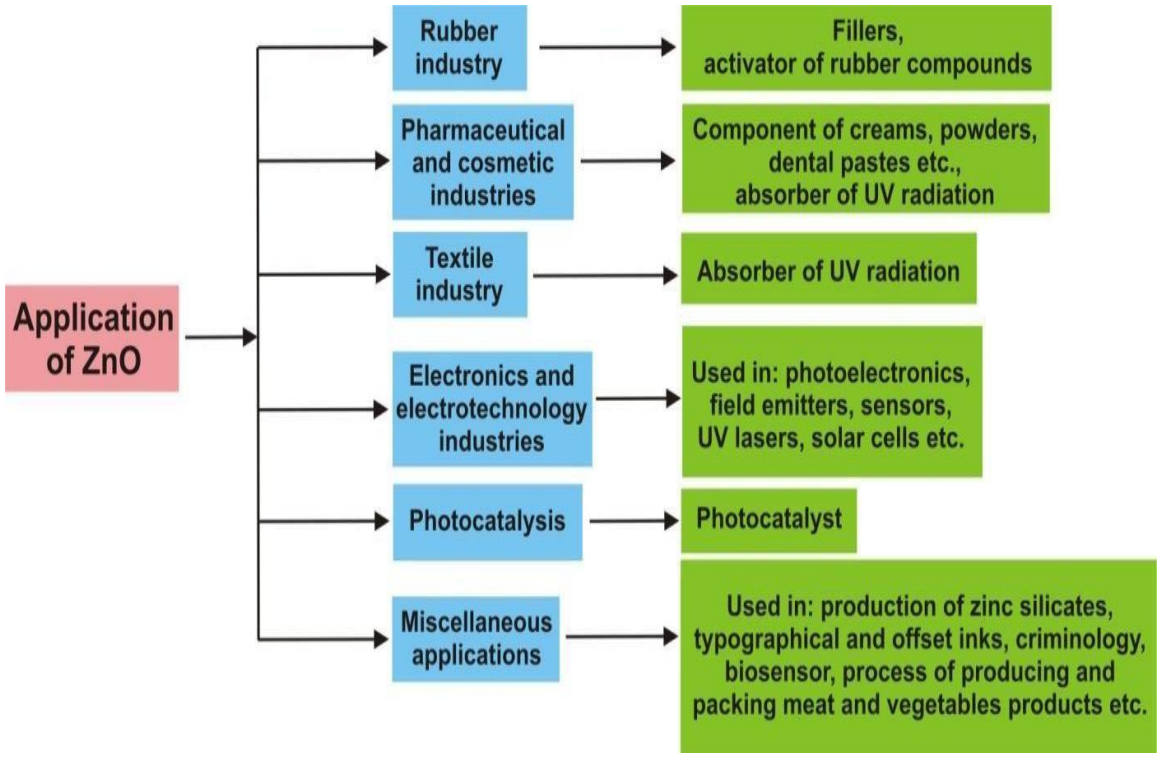

Fig I.6 Schematic presentational the application of ZnO mentioned in the text.

I.5 Thin films preparation Techniques:

1.5.1 Physical vapor deposition (PVD):

The various techniques used in this method are evaporation, sputtering, pulsed laser deposition and molecular beam epitaxy.

I.5.1.1 Thermal evaporation by resistive heating:

Thermal evaporation is the most widely used technique for the preparation of thin films of metals, alloys, and also many compounds, as it is very simple and convenient. Here the only requirement is to have a vacuum environment in which sufficient amount of heat is given to the evaporants to attain the vapor pressure necessary for the evaporation. The evaporated material is allowed to condense on a substrate kept at a suitable temperature. When evaporation is made in vacuum, the evaporation temperature will be considerably lowered and the formation of the oxides and incorporation of impurities in the growing layer will be reduced. Evaporation is normally done at a pressure of 10-5 Torr. At this pressure a straight-line path for most of the emitted vapor atoms is ensured for a substrate to source distance of nearly 10 to 50 cm. The characteristics and quality of the deposited film will depend on the substrate temperature, rate of deposition, ambient pressure, etc. and the uniformity of the film depends on the geometry of the evaporation source and its distance from the source. The deposition by thermal evaporation is simple, convenient and is widely use. [11]

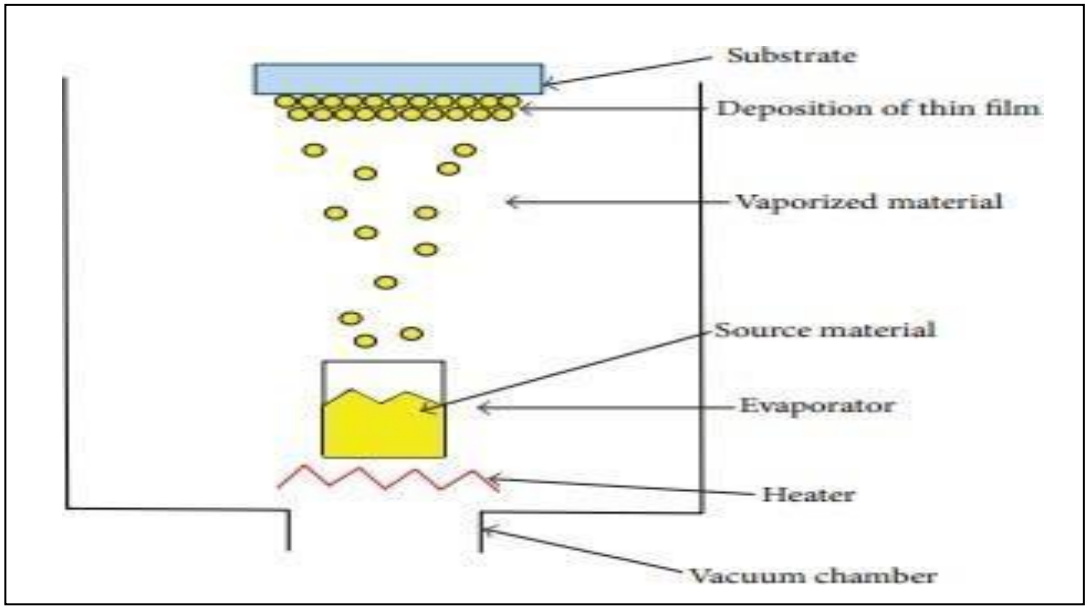

Fig I.7 Schematic of Thermal evaporation by resistive heating

I.5.1.2 Electron beam evaporation:

Electron beam evaporation (EBE) a stream of electrons is accelerated through fields of typically 5–10kV and focused onto the surface of the material for evaporation. The electrons lose their energy very rapidly upon striking the surface and the material melts at the surface and evaporates. That is, the surface is directly heated by impinging electrons, in contrast to conventional heating modes. Direct heating allows the evaporation of materials from watercooled crucibles. Such water-cooled crucibles are necessary for evaporating reactive and in particular reactive refractory materials to avoid almost completely the reactions with crucible walls. This allows the preparation of high purity films because crucible materials or their reaction products are practically excluded from evaporation.

Electron beam guns can be classified into thermionic and plasma electron categories. In the former type the electrons are generated thermionically from heated refractory metal filaments, rods or disks. In the latter type, the electron beams are extracted from plasma confined in a small space.

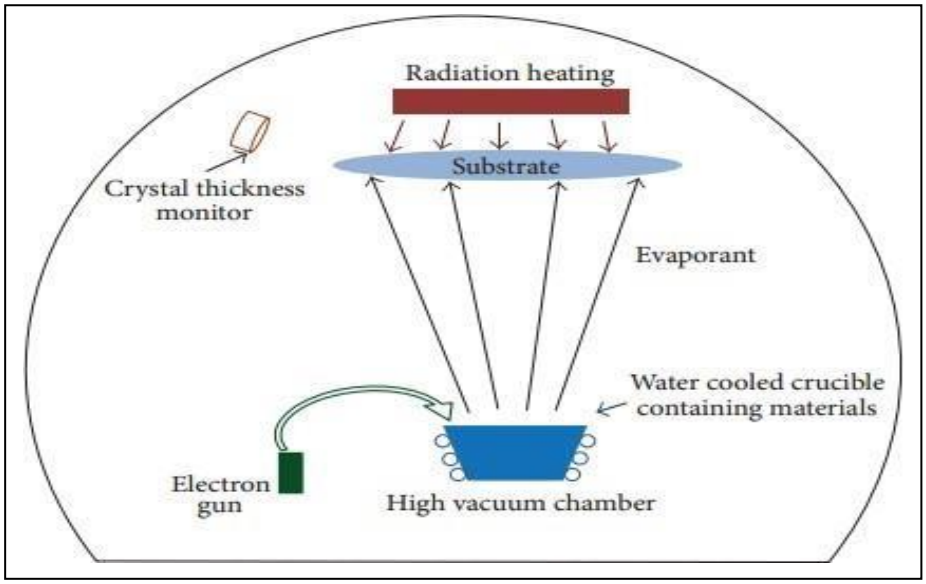

Fig I.8 General diagram of Electron Beam Evaporator [11].

I.5.1.3. Sputtering:

Sputtering is one of the most versatile techniques used for the deposition of transparent conductors when device quality films are required. Sputtering process produces films with better controlled composition, provides films with greater adhesion and homogeneity and permits better control of film thickness. The sputtering process involves the creation of gas plasma usually an inert gas such as argon by applying voltage between a cathode and anode. The target holder is used as cathode and the anode is the substrate holder. Source material is subjected to intense bombardment by ions. By momentum transfer, particles are ejected from the surface of the cathode and they diffuse away from it, depositing a thin film onto a substrate. Sputtering is normally performed at a pressure of 10^{-2} –10^{-3} Torr.

Normally there are two modes of powering the sputtering system; DC and RF biasing. In DC sputtering system a direct voltage is applied between the cathode and the anode. This method is restricted for conducting materials only. RF sputtering is suitable for both conducting and non-conducting materials; a high frequency generator (13.56 MHz) is connected between the electrodes of the system. Magnetron sputtering is a process in which the sputtering source uses magnetic field at the sputtering target surface. Magnetron sputtering is particularly useful when high deposition rates and low substrate temperatures are required. [11]

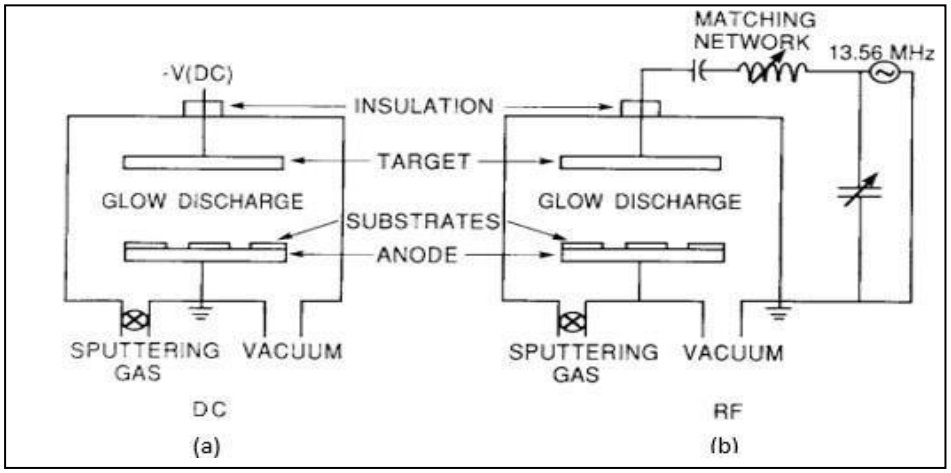

Fig.I.9 Schematics of simplified sputtering systems: (a) DC, (b) RF

I.5.1.4 Molecular Beam Epitaxial (MBE):

Selected elements, e.g. Ga, As, Al, etc. are heated in vacuum furnaces called effusion cells. Evaporated atoms and molecules leave the cells in collimated beams and impinge on a heated surface of a monocrystalline wafer. Here they enter different processes (physical adsorption, chemisorption, migration), undergo transformation (dissociation, association, etc.) and at last form a monocrystalline lattice. Molecular beams can be interrupted by shutters placed in front of the cell orifices. By this way it is possible to change composition and properties of grown layers. Some cells usually contain dopant elements (Si and Be for n- or p doping in GaAs) which control the type of electrical conductivity. Growth process is realized in ultra-high vacuum chamber with ultimate pressure in the order of 10-11 mbar. The chamber is equipped with a number of effusion cells, with manipulator for sample heating (0–1000 C°) and azimuthally rotation, with an electron gun and screen for RHEED (reflection high-energy electron diffraction) and other accessories. Inner chamber walls are surrounded by cryopannels, which are cooled by liquid nitrogen (-197 C°) during the growth). [11]

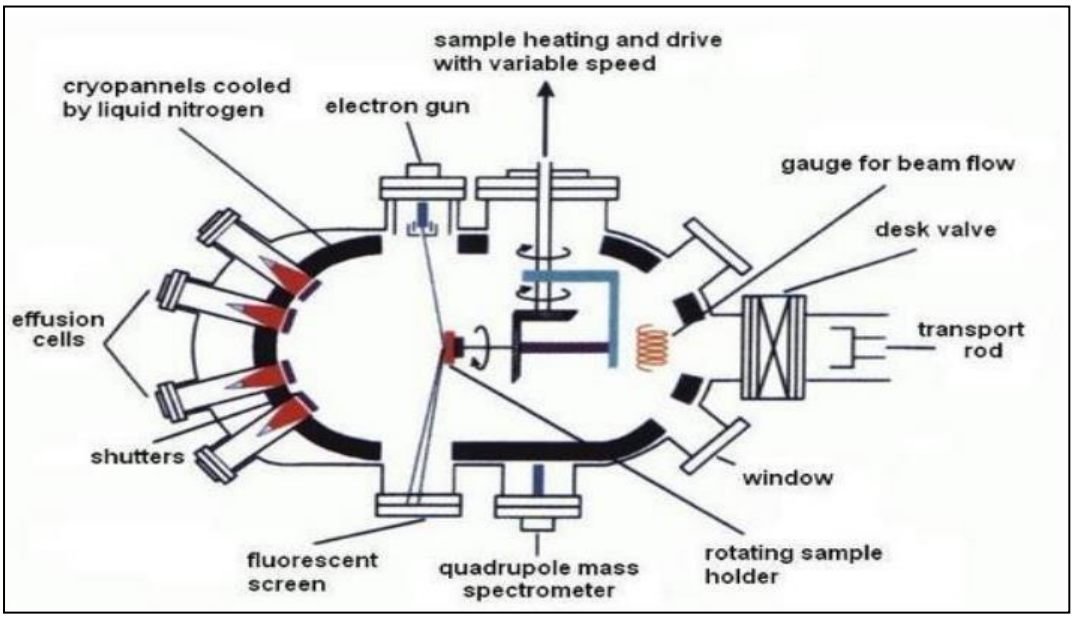

Fig I.10 The MBE growth chamber design, the sample is fixed in the chamber center on a rotating holder

I.5.2 Chemical vapor deposition:

CVD processes are grouped together under the common name “Chemical Vapor Deposition” and are synthetic techniques based on the chemical reaction of one or more chemicals. Several gas-phase precursor volatile compounds that react chemically to form a solid film deposited on a heated substrate. This chemical reaction requires a substrate heat

supply, either by joule effect, induction, thermal radiation or laser. In these techniques, several parameters come into play (temperature, pressure, presence of plasma, nature of volatile products, etc.). The temprature of the substrate provides the activation energy needed to trigger the chemical reaction. This temperature is often very high, ranging from 800 °C to 1000 °C. Among the methods of synthesis are distinguished [12].

There are a wide range of techniques that fall under the CVD category and ultimately differ in one parameter [13].

- Metal-organic chemical vapour deposition (MOCVD) is a specific type of CVD that utilizes metal-organic precursors.
- Metal-organic vapour phase epitaxy (MOVPE) or organometallic vapour phase epitaxy (OMVPE) is an MOCVD process that produces single crystal films on single 3crystal substrates from metal-organic precursors.
- Plasma-assisted or plasma-enhanced CVD (PECVD) is a technique in which electrical energy rather than thermal energy is used to initiate homogeneous reactions for the production of chemically active ions and radicals that can participate in heterogeneous reactions, which, in turn, lead to layer formation on the substrate.
- Atomic layer chemical vapour deposition (ALCVD), sometimes called atomic layer epitaxy (ALE), is a modification of the CVD process in which gaseous precursors are introduced sequentially to the substrate surface and the reactor is purged with an inert gas, or evacuated, between the precursor pulses.
- Chemical beam epitaxy (CBE) is high vacuum CVD technique that uses volatile metal-organic precursors and gaseous co-precursors [7].

References

[1] Babar, A. R., Shinde, S. S., Moholkar, A. V., Bhosale, C. H., & Rajpure, K. Y. Structural and optoelectronic properties of sprayed Sb: SnO2 thin films: Effects of substrate temperature and nozzle-to-substrate distance. Journal of Semiconductors, 32(10), 102001. (2011).

[2] Minami, T. Transparent conducting oxide semiconductors for transparent electrodes. Semiconductor science and technology, 20(4), S35. (2005).

[3] Benkheta, Y. Elaboration and characterization of thin layers of zinc oxide (ZnO) deposited by ultrasonic spray for photovoltaic and optoelectronic applications (PhD Thesis University Mohamed Khider of Biskra). (2019).

[4] Ellmer, K., Klein, A., & Rech, B. (Eds.). Transparent conductive zinc oxide: basics and applications in thin film solar cells. (2007).

[5] Behera, J. K. Synthesis and Characterizations of ZnO Nanoparticles (PhD Thesis). (2009).

[6] Fernandes, J. M., Suresh, G., Muniramaiah, R., Maharana, G., Geetha, A., Kovendhan, M., ... & Joseph, D. P. Effect of anionic bromine doping on the structural, optical and electrical properties of spray-pyrolyzed SnO2 thin films. Materials Science and Engineering: B, 282, 115756. (2022).

[7] Bouaichi, F. Deposition and analysis of Zinc Oxide thin films elaborated using spray pyrolysis for photovoltaic applications (PhD Thesis, University Mohamed Khider of Biskra). (2019).

[8] Amraoui F, G. I. The Influence of Calcination Temperature on Properties of Thin films of Zinc-Oxide (ZnO) elaborated by Sol-gel (Dip-coating) Master memory. (2022).

[9] Vyas, S. A Short Review on Properties and Applications of Zinc Oxide Based Thin Films and Devices: ZnO as a promising material for applications in electronics, optoelectronics, biomedical and sensors. Johnson Matthey Technology Review, 64(2), 202-218(2020).

[10] Othmane, M. Synthesis and characterization of Zinc Oxide (ZnO) Thin films deposited by spray pyrolysis for applying: electronics and photonics (PhD Thesis, University Mohamed Khider of Biskra). (2018).

[11] Dahnoun, M. Preparation and characterizationof Titanium dioxide and Zinc oxide thin films via Sol-Gel (spin coating) technique for optoelectronicapplications (PhD Thesis, University Mohamed Khider Biskra). (2020).

[12] Aouina, W. Etude des propriétés structurales, optiques et électriques des oxydes transparents conducteurs nanostructurés de ZnO dopé Al (PhD Thesis, Université Mohamed Boudiaf, M'sila).(2016).

[11] Dahnoun, M. Preparation and characterizationof Titanium dioxide and Zinc oxide thin films via Sol-Gel (spin coating) technique for optoelectronicapplications (PhD Thesis, University Mohamed Khider Biskra). (2020).

[12] Aouina, W. Etude des propriétés structurales, optiques et électriques des oxydes transparents conducteurs nanostructurés de ZnO dopé Al (PhD Thesis, Université Mohamed Boudiaf, M'sila). (2016).

Chapter II:

Spray pyrolysis and characterization methods

The present work is an attempt to summarize the basic types of equipment (SP), the second part of this chapter includes the different techniques and different relationships, which is used to characterize our thin films.

II.1.Spray pyrolysis (SP):

In our work, we choose spray pyrolysis because this thin film deposition method is simple, cost-effective, and a wide choice of precursors can be used. The composition of the film can be easily controlled by the precursor solution. Both, dense and porous structures can be deposited by spray pyrolysis, even on large substrates when scaling up the equipment.

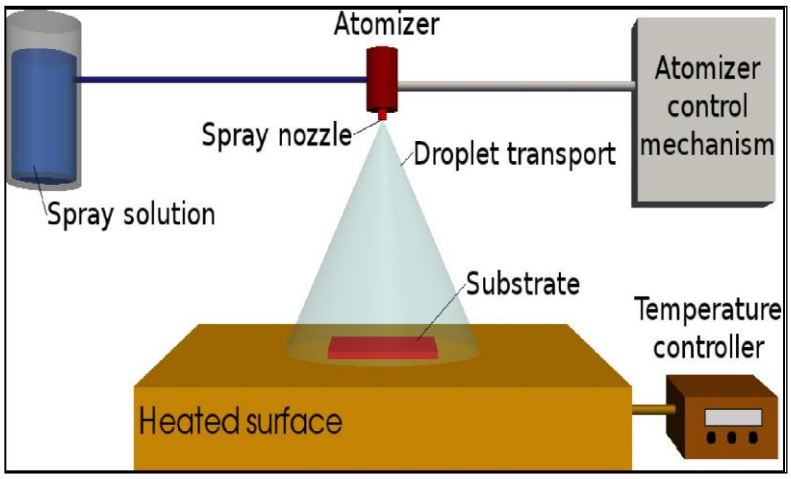

Fig II.1 General schematic of a spray pyrolysis deposition process [1].

The spray pyrolysis technique includes spraying of a solution (usually aqueous, containing soluble salts of the constituent atoms of the desired compound) on a substrate maintained at high temperatures. The sprayed droplets react with the hot substrate surface and undergo pyrolytic (endothermic) decomposition and form cluster of crystallites of the sprayed materials. Thin film deposition using spray pyrolysis can be divided into three main steps: atomization of the precursor solution, transportation of the resultant aerosol and decomposition of the precursor on the substrate.

- **Atomization of the precursor solution**

The film quality and the droplet size of the aerosol are typically set by the atomization technique. The most commonly used techniques for generating droplets are:
1) The pneumatic method: a relatively pressurized air flow carry the solution that contains precursors, the atomization into droplets is composed at the nozzle orifice.
2) Ultrasonic spray method: an ultrasonic wave generator atomizes the solution. The droplet

size is more regular and thinner in ultrasonic spray nozzle than in pneumatic spray. In addition, comparing with the droplet speed in PS, it is low in USP; hence, this may affect the films growth in both methods [2].

- **Transportation of the resultant aerosol**

The droplets have to be moved to the substrate, when aerosol is transported, without composing powder or salt particles. The mechanism of film growth was investigated bySears et al [3]. They discussed the effect of forces that determine the path of the droplets and the evaporation. Also, they suggested a model of a film growth taking into consideration the gravitational, electric thermophoretic and Stokes forces (Fig.II.2).

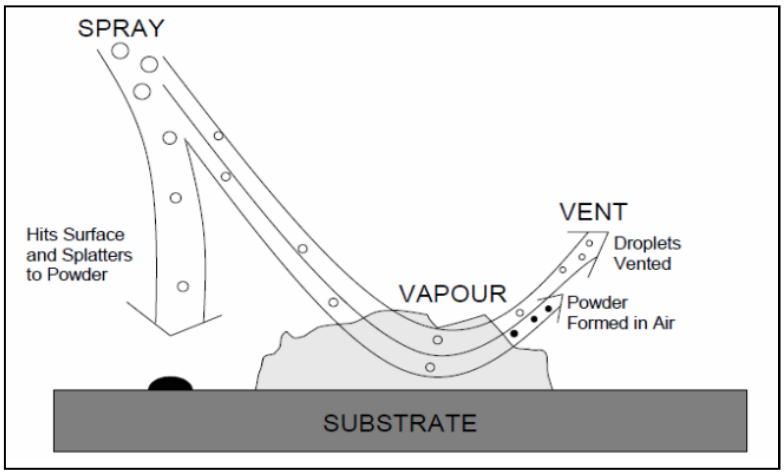

Fig II.2. Schematic of aerosol transport by Sears et al. [4]

- **Decomposition of Precursor:**

During decomposition of the precursor, several operations take place simultaneously (evaporation of residual solvent, spreading of the droplet, and salt decomposition). They are identified in Fig.II.3.

Many processes occur simultaneously when a droplet hits the surface of the substrate: evaporation of residual solvent, spreading of the droplet, and salt decomposition. Many models exist for the decomposition of a precursor. At low substrate temperature (processA), the droplets plashes onto the substrate surface and decomposes.At higher temperatures (processB) the solvent evaporates completely during the flight of the droplet and dry precipitate hits the substrate, where decomposition occurs. At even higher temperatures (more than the latter case), the solvent also evaporates before the droplet reaches the substrate. Then the solid precipitate melts and vaporizes without decomposition and the vapor diffuses to the substrate to undergo a CVD process (process C).At the highest temperatures (processD), the precursor vaporizes before it reaches the substrate, and consequently the solid particles are

formed after the chemical reaction in the vapor phase.

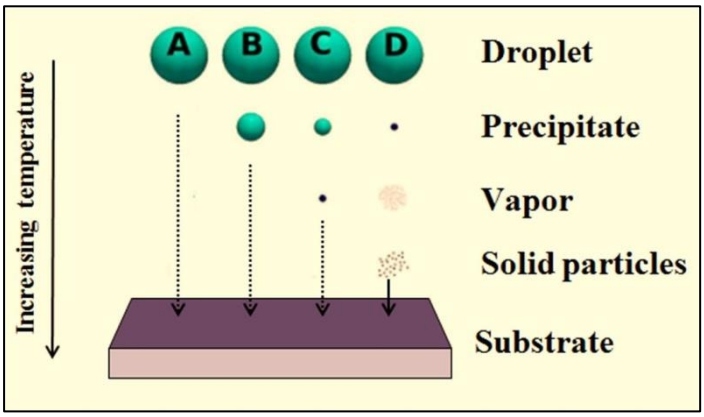

Fig II.3: Description of the deposition processes initiated with increasing substrate temperature.

II.3 .ZnO characterization techniques:

II.3.1 Thickness measurement:

II.3.1.1 Weight Difference Method:

The film thickness is an important parameter in the study of the film properties. Among various techniques that evaluate the film thickness, one can write the weight difference technique. It is simple and useful .The thickness "t" can be calculated as follows [4]

$$t = \frac{\Delta m}{s.\rho} \qquad \text{(II.1)}$$

m: the mass of the film

s: the substrate area

ρ: the density of the material in the bulk form.

The mass of the film has been measured by using a single pan microbalance.

II.3.2. X-ray diffraction (XRD):

The X rays diffraction is carried out to study the crystalline quality of the ZnO thin films. It is a simple and non-destructive analysis technique, which provides means to identify

different phases and their distribution in the sample, texture, evaluate average grain size, internal stress, etc.

X-rays are electromagnetic waves with wavelength (0.5-50 Å) comparable to atomic separation distances. When propagating through a crystal, the X-rays interact with the lattice (see Fig.II.4) and are diffracted according to the Bragg's law [5, 6, 7]

$$n\lambda = 2d \sin\theta \qquad \text{(II.2)}$$

Where,

d: interlinear spacing

θ: diffraction angle

λ: wavelength of x-ray

n: order of diffraction

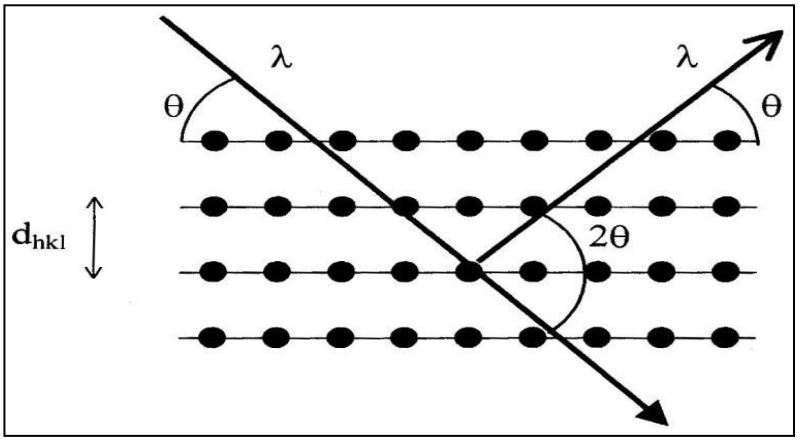

Fig II.4. Interaction of x-rays with planes of atoms [6]

The X-rays diffraction provides a series of information about the crystal structure, orientation, average crystalline size and stress in the films. In this study, we measured the crystalline properties of the films with X-ray diffraction (XRD) using a D8ADVANCE diffractometer (λ=1.5405 Å). The diffraction patterns experimentally achieved are compared with standard powder diffraction files published by the International Centre for Diffraction Data (ICDD)

- **Determination of the crystallite size**

The average crystallite size of the deposits is estimated from the full width at half maximum (FWHM) of the most intense diffraction line by Scherer's formula as follows **[**8, 9, 10**].**

$$G = \frac{(0{,}94\ .\lambda)}{\beta.\ \cos\theta} \qquad \text{(II.3)}$$

G is the size of the grains ([G] = nm)

λ is the wavelength of the beam of X ray.

θ is the angle of diffraction.

β is full width at half maxima of the peak (FWHM) in radians.

It can be calculate the dislocations density using the grains size values according to the following relationship [11, 12]

$$\delta = \frac{1}{G^2} \qquad \text{(II.4)}$$

- **Determination of the lattice parameters**

The lattice parameters (a=b, c) have been determined by the equation below **[**13**]**

$$a = \frac{\lambda}{\sqrt{3}\ \sin\theta(100)} \qquad \text{(II. 5)}$$

$$c = \frac{\lambda}{\sin\theta(002)} \qquad \text{(II. 6)}$$

a and *c*: the lattice parameters

θ is the angle of diffraction.

- **Strain determination:**

The stresses directly shift the diffraction peaks according to the biaxial stress model. The deformation along the c axis is given by: [14, 15, 16]

$$\varepsilon = \frac{C-C0}{C0} \qquad \text{(II.7)}$$

C_0:The standard value of the crystal dimension

C: The crystal dimension of the slide

- **Stress measurement**

The calculation of the mean film stress $\sigma_{film}$is based on the biaxial strain model. The strain ε_{zz}in the *C*-axis, i.e., perpendicular to the substrate surface (our case), the following

formula is used, which is valid for a hexagonal lattice. The internal stress in ZnO thin films is given by the following relationship [14]:

$$\sigma_{film} = \left(2C_{13} - \frac{(C_{11}+C_{12})C_{33}^{film}}{C_{13}}\right)\varepsilon_{zz} \qquad \text{(II.8)}$$

Avec : $C_{33}^{film} = \frac{0.99C_{33}^{cristal}}{(1-e_{zz})^4}$ et $\varepsilon_{zz} = \frac{c_{film}-c_0}{c_0}$

$C_{11} = 209.7GPa,$

$C_{12} = 121.1\ GPa,$

$C_{13} = 105.1\ GPa,$

$C_{33} = 210.9\ GPa$

$c_0 = 5{,}206$ Å

II.3.3. Scanning electron microscope SEM:

The scanning electron microscope (SEM) is a type of electron microscope that images the sample surface by scanning it with a high-energy beam of electrons in a raster scan pattern. The electrons interact with the atoms to make the sample producing signals that contain information about the surface of the sample, composition and other properties of the ZnO thin films.

The SEM uses electrons instead of light to form an image. A beam of electrons is produced at the top of the microscope by heating of a metallic filament. The electron beam follows a vertical path through the column of the microscope. It makes its way through electromagnetic lenses which focus and direct the beam down towards the sample. Once it hits the sample, other electrons such as backscattered or secondary are ejected from the sample (see Figure II.5) [17].

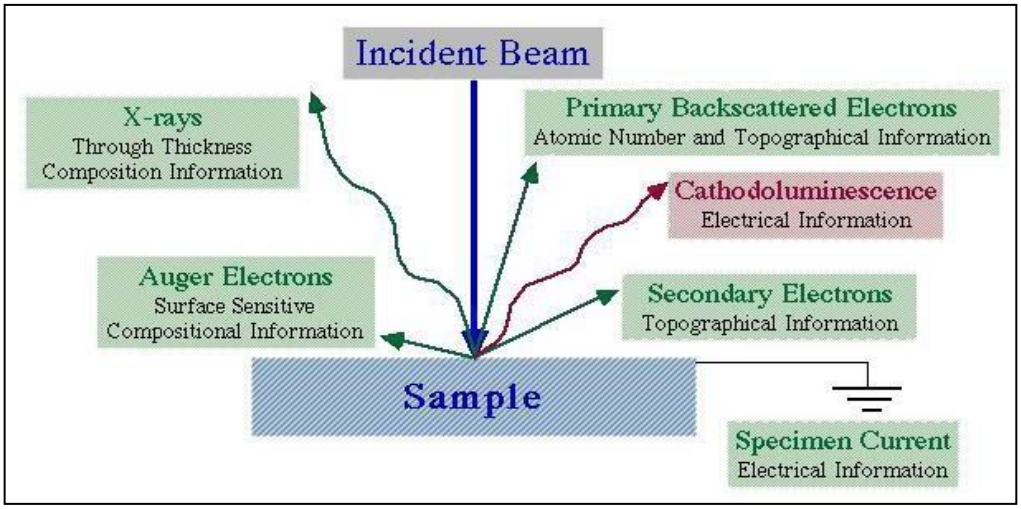

Fig. II.5: Illustration of electron-specimen interactions in SEM [8]

II.3.4Measurement of optical properties:

- **UV-Vis spectroscopy:**

The spectrophotometry is the quantitative measurement of transmission or reflection properties by material as a function of wavelength of the incident radiation. We measured the sample transmittance spectra with a dual beam UV-VIS-NIR scanning spectrophotometer of type SHIMADZU UV-3101 PC. The principle of this process is shown in Fig II.6

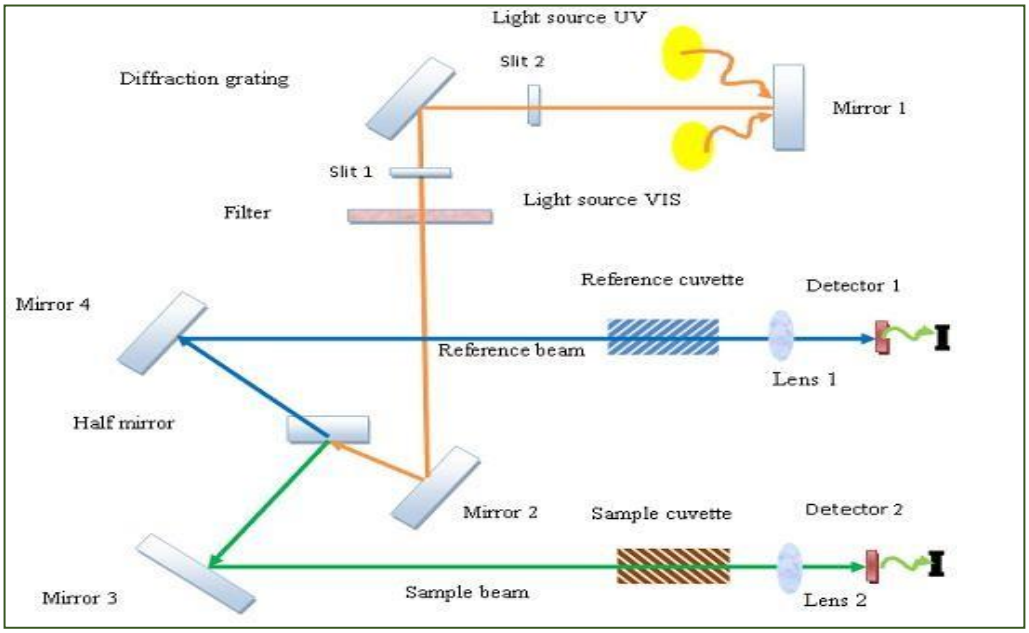

Figure II.6 .The principle of operation of UV-visible [1].

The light is moved from the source by optics in the instrument and hits the surface of the sample in which the light is distributed into three parts: Transmission (*T*), Reflection (*R*) and Absorption (*A*). The total of these three parts must be equal to the input light. As a result, if we

esteem the sum of input light is1, one can write:

$$R + A + T = 1 \qquad \text{(II.9)}$$

The amount of light crossing a sample (*I*) comparing it with that of light before crossing the sample (I_0). The ratio (I/I_0) is known as the transmittance and generally expressed as a percentage (*T %*). The experimental data (the transmittance (*T*)) is used to calculate the absorbance (*A*), absorption coefficient (α), refractive index (*n*), band gap (*Eg*) and film thickness (*t*).

- **Absorption coefficient**

The absorption coefficient (α) of the films, presented by Beer-Lambert relation, hypothesizing that the reflected light is negligible [1]:

$$\alpha = \frac{1}{t}\ln\frac{100}{T\%} \qquad \text{(II.10)}$$

Where*:*

α: the absorption coefficient

t: the thickness of the film

T: the transmittance.

- **Band gap energy:**

In the strong absorption region, the photons induce electronic transitions from the valence band to the empty energy states in the conduction band. By using Tauc relationship [18, 19, 20], we can evaluate in this area the value of the optical band gap:

$$(\boldsymbol{\alpha h\nu}) = \boldsymbol{A(h\nu - Eg)^m} \qquad \text{(II.11)}$$

Where *h* is photon energy and *Eg* is the optical gap m and *A* are constants; m describes the optical type of transition and has values of 2, 1/2 (2 for authorized direct transitions and 1/2 for permissible indirect transitions). Fig II.7 shows the typical $(\alpha h\nu)^2$ versus $h\nu$plots of the ZnO thin films. The linear dependence of $(\alpha h\nu)^2$ on $h\nu$indicates that the film is direct transition type semiconductor.

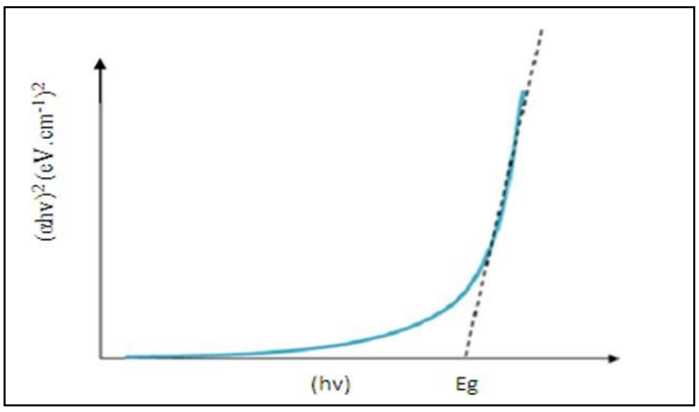

Fig II.7. Determination of Eg.

- **Urbach energy (Eu):**

Urbach energy is usually explained as the width of the band tail because of the localized states in the typical band gap that is associated with the disordered or low crystalline materials. The spectral dependence of the absorption coefficient (α) and photon energy (hν) is called "Urbach empirical rule" which can be expressed through the following relation [21]:

$$\alpha(h\nu) = \alpha_0 \exp\frac{h\nu}{E_U} \qquad \text{(II.12)}$$

When we take the logarithm of both extremities of the previous equation, hereafter, one may obtain a straight line equation. It is presented as follows:

$$\ln \alpha = \ln \alpha_0 \frac{h\nu}{E_U} \qquad \text{(II.13)}$$

By plotting Lnα as function of *hν*, we can determine E_U value as the reciprocal of the linear part slope (Fig. II.8)

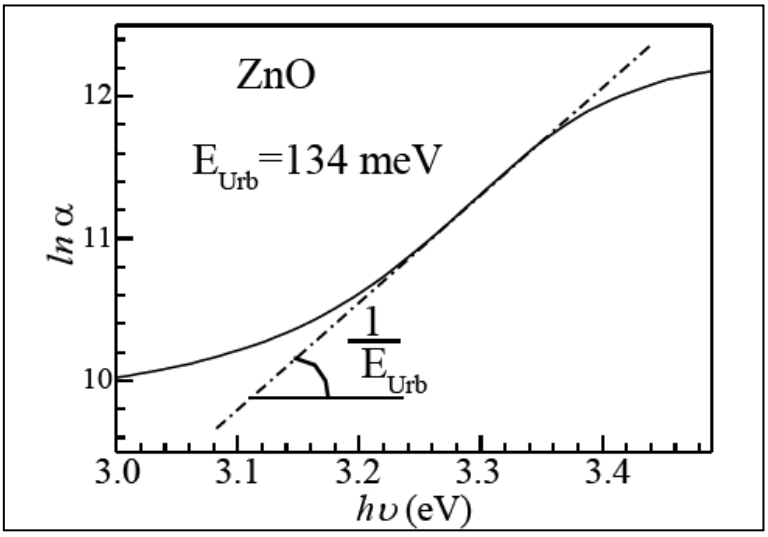

Fig II.8 Determination of Urbach energy (E_u).

II.3.5 Electrical characterization:

- **Four probes technique:**

For electrical resistance measurement for thin films, the four -probe method is the most extensively used in thin films. This technique forces a fixed current through the sample, using two outer probes as shown in the figure, and measures the resulting voltage between the two inner probes.

Method is used when the specimen is in parallelepiped form of a thin wafer, such as a thin semiconductor material deposited on a glass substrate. The sample is millimeter in size and having a thickness (t). At similar distance (S) between of four probes arranged linearly in a straight line. [17]

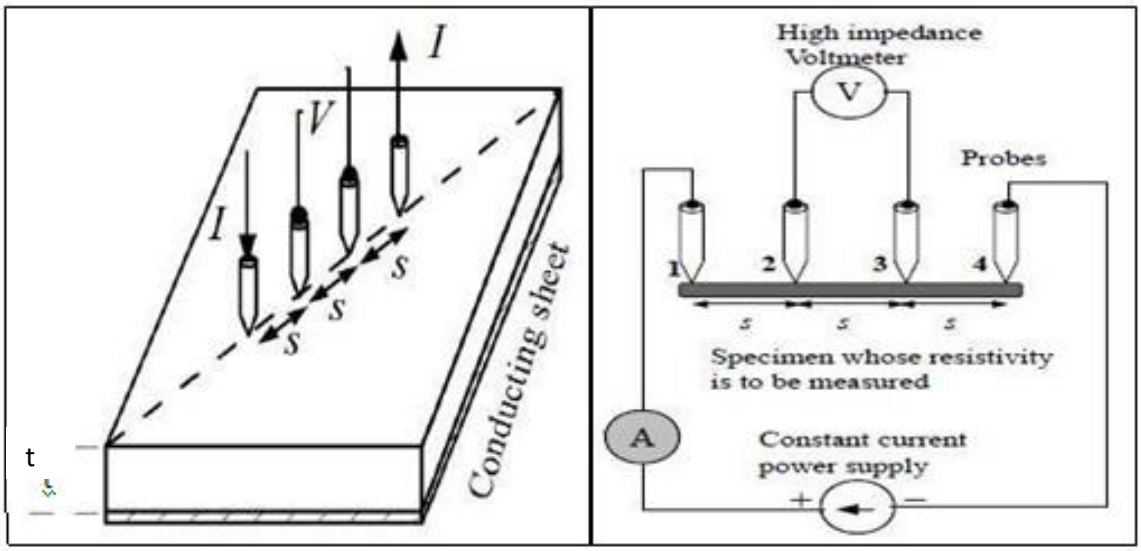

Fig II.9: Schematic Diagram showing the four-point probe technique.[17]

$$\rho = \left[\frac{\pi}{\ln 2}\frac{V}{I}\right].t = R_S.t \qquad \text{(II.14)}$$

$$R_S = 4.53\frac{V}{I} \qquad \text{(II.15)}$$

Where Vis the potential difference between inner probes, I is the current through the outer pair of probes and Rs is the sheet resistance.

References

[1] Sanchez-Juarez, A., Tiburcio-Silver, A., & Ortiz, A. Properties of fluorine-doped ZnO deposited onto glass by spray pyrolysis. Solar energy materials and solar cells, 52(3-4), 301-311. (1998).

[2] Bennaceur, K. Elaboration and characterization of SnO2: In thin films deposited by spray pyrolysis technique (PhD Thesis, University Mohamed Khider Biskra). (2020).

[3] Sears, W. M., & Gee, M. A. Mechanics of film formation during the spray pyrolysis of tin oxide. Thin solid films, 165(1), 265-277. (1988).

[4] Kherchachi, I. B., Attaf, A., Saidi, H., Bouhdjar, A., Bendjdidi, H., Youcef, B., & Azizi, R. The synthesis, characterization and phase stability of tin sulfides (SnS2, SnS and Sn2S3) films deposited by ultrasonic spray. Main Group Chemistry, 15(3), 231-242. (2016).

[5] Sofiani, Z. Contributions à l'étude des propriétés optiques non linéaires de nanoparticules en couches minces à base de ZnO (PhD Thesis, Université d'Angers). (2007).

[6] Benramache, S. Elaboration et caractérisation des couches minces de ZnO dopées cobalt et indium (PhD Thesis, University Mohamed Khider Biskra). (2012).

[7] Moustaghfir, A. Elaboration et caractérisation de couches minces d'oxyde de zinc. Application à la photoprotection du polycarbonate (PhD Thesis, Université Blaise Pascal-Clermont-Ferrand II). (2004).

[8] Sali, S., Boumaour, M., Kermadi, S., Keffous, A., & Kechouane, M. Effect of doping on structural, optical and electrical properties of nanostructure ZnO films deposited onto a-Si: H/Si heterojunction. Superlattices and Microstructures, 52(3), 438-448. (2012).

[9] Baghdad, R., Lemée, N., Lamura, G., Zeinert, A., Hadj-Zoubir, N., Bousmaha, M., ... & Zellama, K. Structural and magnetic properties of Co-doped ZnO thin films grown by ultrasonic spray pyrolysis method. Superlattices and Microstructures, 104, 553-569. (2017).

[10] Prathap, P., Devi, G. G., Subbaiah, Y. V., Reddy, K. R., & Ganesan, V. Growth and characterization of indium oxide films. Current Applied Physics, 8(2), 120-127. (2008).

[11] Derbali, A., Attaf, A., Saidi, H., Aida, M. S., Benamra, H., Attaf, R., ... & Derbali, L. Br doping effect on structural, optical and electrical properties of ZnS thin films deposited by ultrasonic spray. Materials Science and Engineering: B, 268, 115135. (2021).

[12] Kayani, Z. N., Shah, I., Zulfiqar, B., Riaz, S., Naseem, S., & Sabah, A. Structural, optical and magnetic properties of nanocrystalline Co-Doped ZnO thin films grown by Sol–Gel. Zeitschrift für Naturforschung A, 73(1), 13-21. (2017).

[13] زوبيري بلا ل. د راسة خصا ئص الشرائح الرقيقة لأكسيد الزنك المحضرة بطريقة الرش بالهواء المضغوط انطلاقا من مصادر مختلفة للزنك (مذكرة ماستر). (2022).

[14] Rahal, B., Boudine, B., Larbah, Y., Guerbous, L., Sebais, M., Halimi, O., & Siad, M. Sol-gel synthesis and nanostructured semiconductor analysis of undoped and Cd-doped ZnO thin films. Optik, 169, 303-313. (2018).

[15] Lehraki, N., Attaf, A., Aida, M. S., Attaf, N., Othmane, M., & Bouaichi, F. Effect of different Zinc precursors in Structural and Optical properties of ZnO thin films. arXiv preprint arXiv:2003.08487. (2020).

[16] Rafique, S., Kasi, A. K., Kasi, J. K., Bokhari, M., & Shakoor, Z. Fabrication of Br doped ZnO nanosheets piezoelectric nanogenerator for pressure and position sensing applications. Current Applied Physics, 21, 72-79. (2021).

[17] Othmane, M. Synthesis and characterization of Zinc Oxide (ZnO) Thin films deposited by spray pyrolysis for applying: electronics and photonics (PhD Thesis, University Mohamed Khider Biskra). (2018).

[18] Asikuzun, E., Ozturk, O., Arda, L., & Terzioglu, C. Preparation, growth and characterization of nonvacuum Cu-doped ZnO thin films. Journal of Molecular Structure, 1165, 1-7. (2018).

[19] Fouchet, A. Croissance et caractérisations de films minces de ZnO et ZnO dopé cobalt préparés par ablation laser pulsé (PhD Thesis, Université de Caen). (2006).

[20] Noua, A., & Guemini, R. Preparation and characterization of thin films nanostructures based on ZnO and other oxides. (2019).

[21] Benramache, S., Benhaoua, B., & Belahssen, O. The crystalline structure, conductivity and optical properties of Co-doped ZnO thin films. Optik, 125(19), 5864-5868. (2014).

Chapter III:

Experimental Part and Discussion

III.1 Introduction:

In this chapter, we present the steps used for the technique of deposition of thin films of zinc oxide by pneumatic spray pyrolysis which is a simple and inexpensive technology compared to other methods, and the device can be produced locally.

We will discuss in this chapter too the deposition of undoped and bromine doped zinc oxide thin films, using the pneumatic spray pyrolysis technique, to study the doping rates on the structural, optical and electrical properties of the thin films.

III.2 Experimental method:

III.2.1 Pneumatic spray pyrolysis technique:

This work was fulfilled in thin films laboratory (LPCMA) at the University of Biskra. The technique employed to deposit Zno: Br thin film is pneumatic spray pyrolysis (PSP). Fig.III.1 shows the device of PSP which set up to prepare thin films.

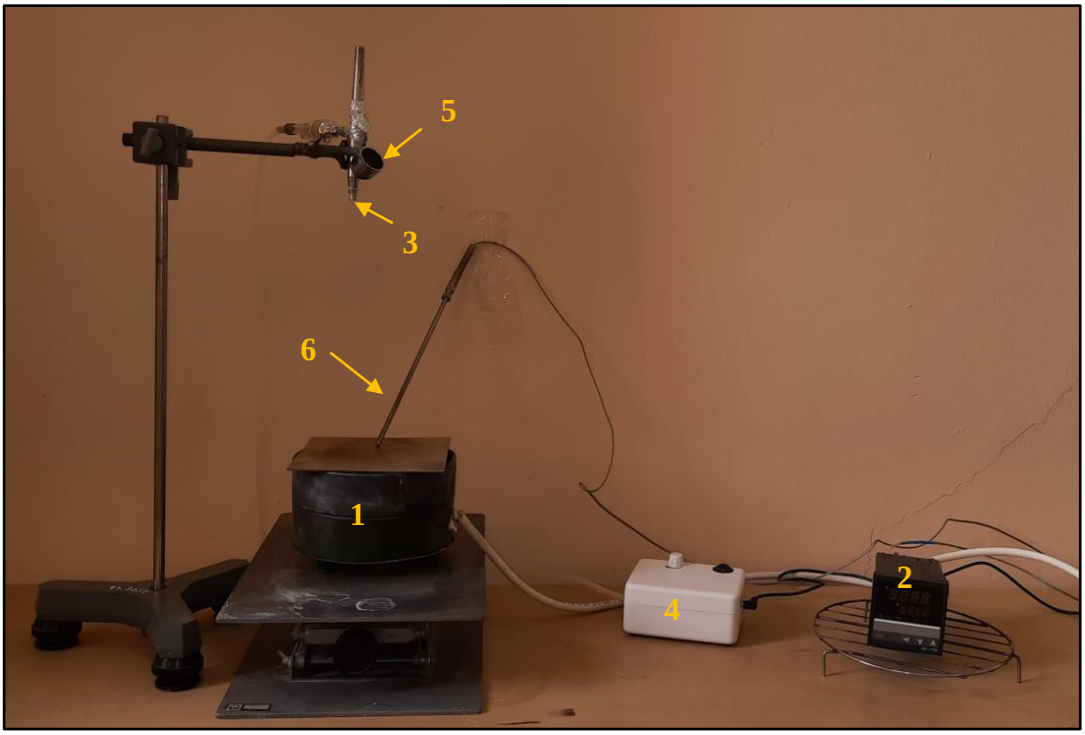

Fig III.1 Image of the device used for deposition

Deposition device components:

1. Sample holder and heating plate.
2. Temperature regulator connected with a thermocouple to check the temperature.
3. Atomizer to decay the solution to fine droplets.
4. Air Compressor.
5. Solution vial.
6. Thermocouple

III.2.2 Preparation of substrates and spray solutions:

III.2.2.1 Preparation of substrates:

a. Choice of the substrate:

The substrate is an essential element in any structure involving a film. It plays a crucial role as a principal material in thin film growth. In this work, we chose the glass slides (25×25mm2) as substrates. The reasons behind this choice are:

- ✓ Glass has a thermal expansion value that is very close to zinc oxide's (ZnO) thermal expansion value.
- ✓ Because of the glass's high transparency, which corresponds to photoanalysis of thin films.
- ✓ Its price is inexpensive.

b. Cleaning the substrate:

The purity and the surface state are the main responsible of the adherence and the quality of the thin films. Therefore, the way of cleaning the substrates surface is as follows:

- The use of pen with diamond point for cutting the substrates.
- The process of cleaning should be done with soap solution.
- Rinsing with the distilled water
- Rinsing with acetone during 5 min.
- Rinsing with distilled water.
- Rising with ethanol during 5 min.
- Cleaning in distilled water bath.
- Drying using a drier.

III.2.2.2 Preparation of solutions:

In this study, we prepared ZnO thin films doped with Br in varying proportions (0%, 2%, 4%, 6% and 8%). The precursors used are: zinc acetate ($CH_6O_4Zn.H_2O$) and the doping source is potassium bromine (KBr). Both precursors are dissolved in distilled water using a magnetic stirrer at 60 °C. A little HCl is added to the solutions to speed up the reaction. To deposition the thin films, we first dry the glass bases, then heat the support to 400 °C, and finally deposition the thin films for 5 minutes.

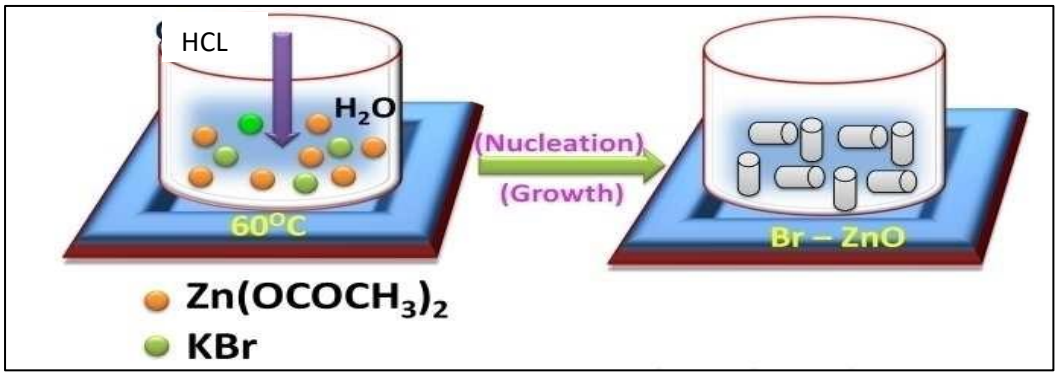

Fig III.2 The solution of zinc oxide Br doping

Fig. III.3 Image of the magnetic mixer

Table III.1 Shows the experimental conditions for generating zinc oxide (ZnO:Br) thin films

The dissolved substance.	$C_4H_6O_4Zn_2H_2O$
The solvent.	Distilled water
Concentration of the solution (mol / l).	0.1
Distance the opening of the bottle from the substrate .(cm)	13
Substrate temperature (° C).	400
Duration of spraying.(min)	5
Doping concentration (Br wt%)	0, 2, 4, 6 and 8

❖ **Properties of the used elements**

Table III.2. Physical and chemical properties of zinc acetate and KBr [1].

zinc acetate		Potassium Bromine (KBr)	
Exterior	White crystalline solid	Exterior	white crystalline powder
chemical formula	$C_4H_6O_4Zn._2H_2O$	Molecular weight of KBr	119.002 g/mol
Volumetric mass.	1,735 g/cm	Density of KBr	2.74 g/cm^3
molar mass	219.5 g/mol	Melting point of KBr	734 °C
Melting temperature	237 °C	Boiling point of KBr	1,435 °C
Solubility	Soluble in water and methanol	Solubility	Soluble in water

III.2.2.3 Deposition of thin films

We put the substrate on an electric resistance linked to a temperature controller. The temperature is gradually increased from the room temperature to a chosen one. Hence, the solutions were sprayed over the hot substrate in the form of fine droplets. Upon reaching the heated surface, these droplets subject pyrolytic decomposition to form a film on the substrate surface, which provides the thermal energy to the decomposition and subsequent recombination.

III.3 Results and discussions:

Following the deposition of thin films in order to obtain samples with high transparency in the visual range and good conductivity by doping zinc oxide with bromine in various concentrations.

III.3.1 Growth rate of the films:

The growth rate was calculated by dividing the films thickness by the deposition time, we used the weight difference technique to calculate the thickness (t). Table (III.3) shows the thickness of the films for the doping.

Table III.3: Thickness of zinc oxide thin films undoped and Br doped ZnO.

Br (%)	0	2	4	6	8
t(nm)	350	570	445	285	320
Growth rate (Å/sec)	11.66	19	14.83	9.5	10.66

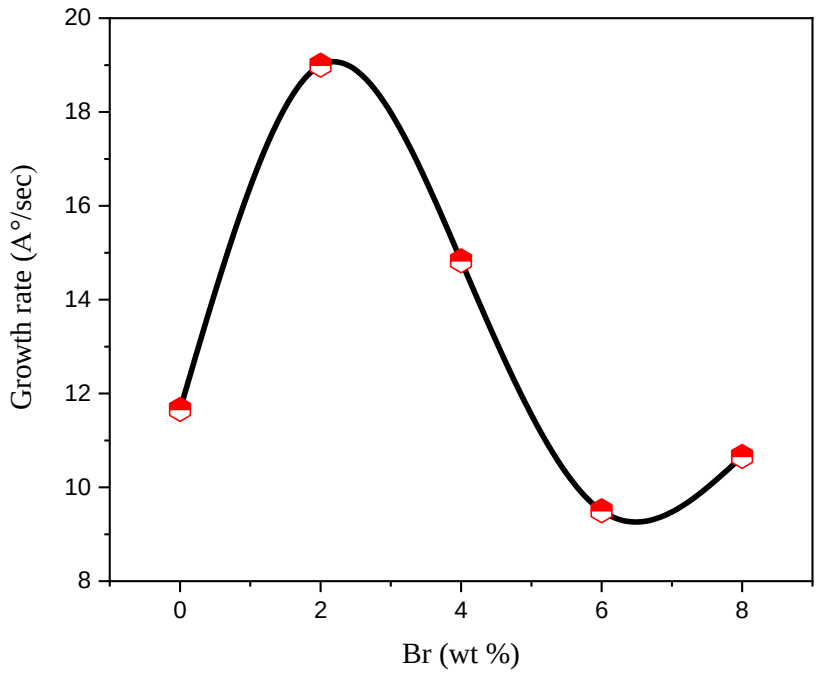

Fig III.4 Variation of Growth speed of bromine-doped zinc oxide thin films.

Fig (III.4) shows the evolution of the growth rate of the films in terms of doping. Usually the growth rate indicates the amount of material deposited on the substrate, so we note that the thin films

of zinc oxide doped with 2% of bromine have the highest growth rate 19 (Å/sec), and the lowest growth rate with 6% is 9.5 (Å/sec). We mention that the weight difference method has a great uncertainty that may affect the results obtained.

III.3.2 Structural study:

The XRD patterns of undoped and doped ZnO at various doping (Br) concentrations (2%, 4%, 6%, 8%.wt) are shown in Fig (III.5).

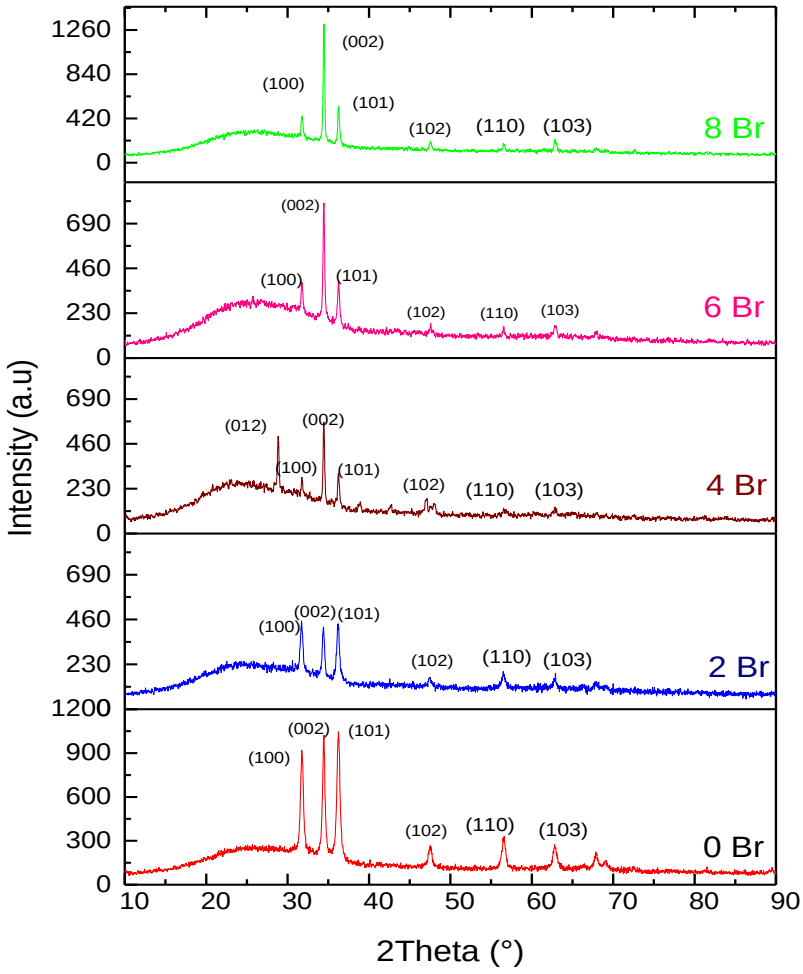

Fig.III.5 XRD patterns obtained from ZnO thin films with different doping levels Br

All peaks are attributed to the hexagonal wurtzite phase of ZnO (JCPDS Card No. 36-1451) Three very prominent peaks appear at angles 31.44°, 34.44° and 36.29°, which correspond to the (100), (002) and (101) levels, respectively with a preferential growth direction (002) at high doping level.

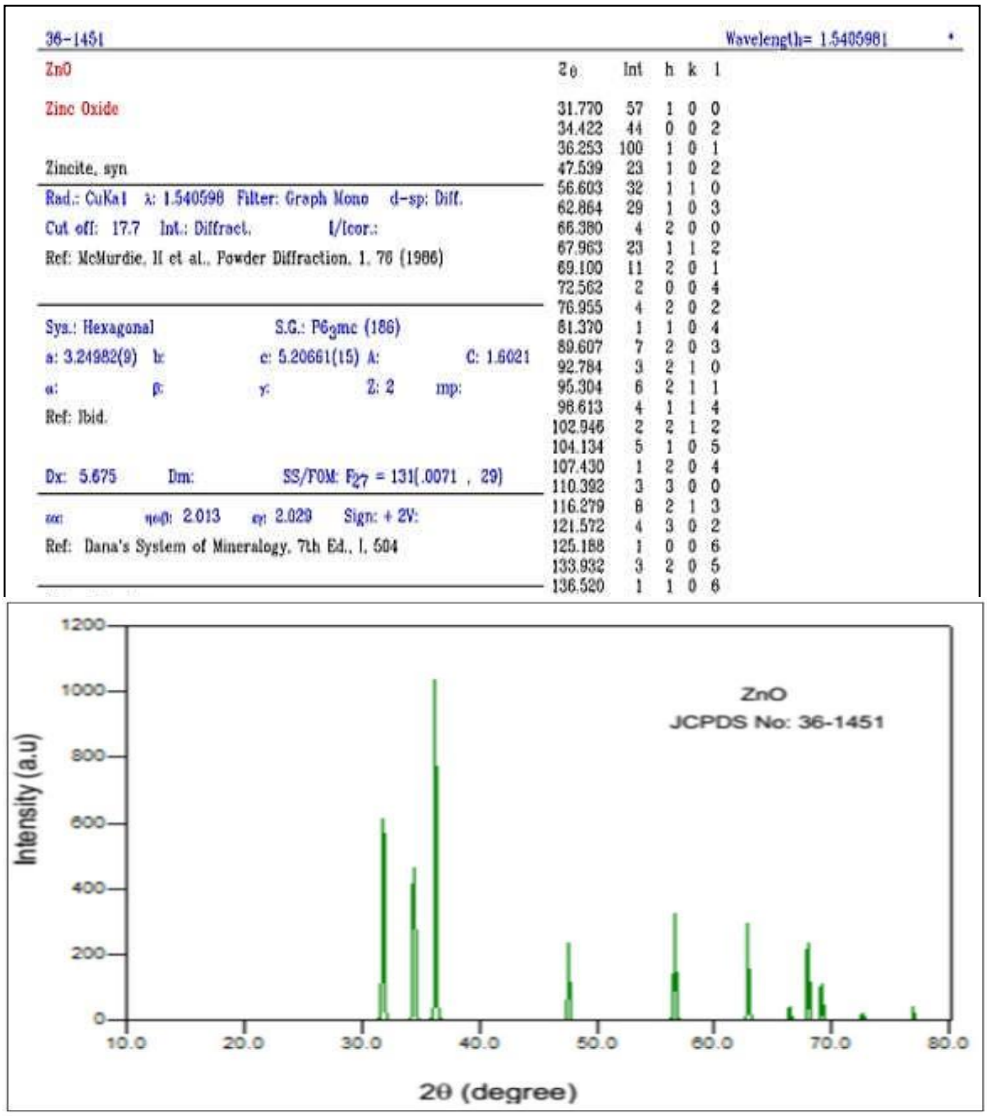

Fig III.6 JCPDS NO. 36-1451

The films crystallize well in the (002) direction where the crystallographic axis "C" is perpendicular to the substrate, This indicates that a large number of atoms move towards the (002) level, which corresponds to the lowest energy for the formation and growth of zinc oxide crystals, as observed in studies [2, 3, 4].

The diffraction intensity of peak (002) increase sharply, indicating that the added amount of Br ions enhances the crystallinity of ZnO films. The increasing peak after Br doping may result due to the fact that Br ions start to substitute Zn ions in the lattice, determining better crystallinity and (002) growth orientation of ZnO films.

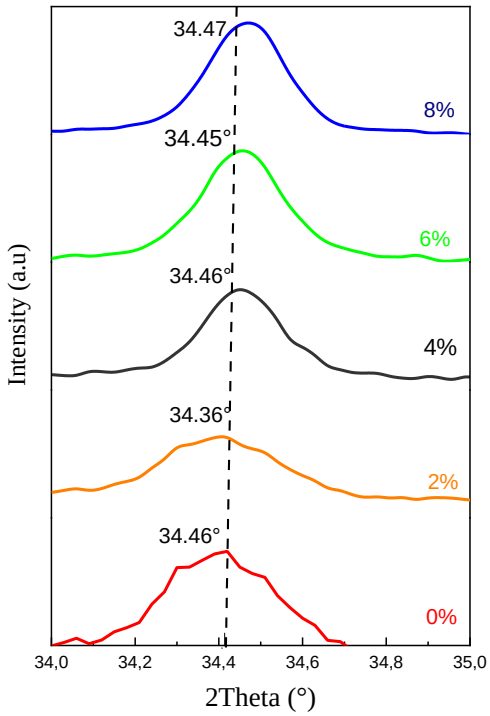

Fig III.7. Main (002) peak shifting of Zno thin films.

As shown in Fig III.7, a slight shift in the position of (002) peak to higher angle was observed, indicating a reduction in the lattice constant (see table III.4), which might be due to the increased oxygen vacancies in the film surface [5].

The variation of grain size and dislocation density as function of the doping concentration, are depicted in the same Fig. III.8. The grain sizes were calculated for the (100), (002) and (101) peaks. It can be seen that the grain size in undoped zinc oxide was 29.91 nm, then it improved by increasing the doping until it reached 47.16 nm at 6%. The G value increases as the doping concentration and this indicates the improvement in crystallinity of the films (as shown by the XRD patterns).

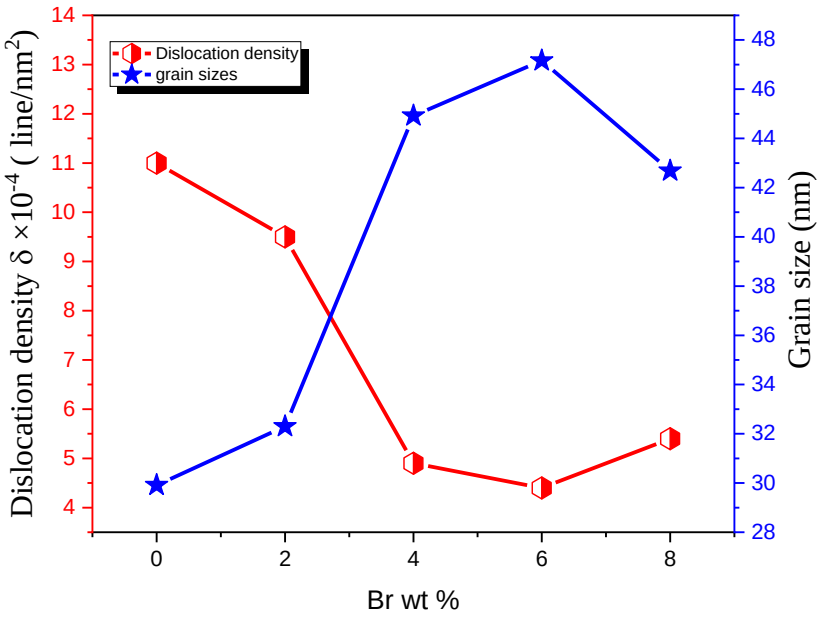

Fig III.8: Grain sizes and dislocation density as functions of Br-doping.

.Furthermore, the dislocation density decrease with the increase of doping concentration ,this reduction is attributed to the improvement of crystalline quality of all the films. Several studies have shown that an increase in the density of dislocations affects the crystal size and thus a decrease in the quality of film formation [6, 7].

The table (III.4) presents the variation of lattice parameters, ‘a’ and ‘c’ of all the samples with Br concentration. The calculated ‘a’ and ‘c’ values are very close to those of the standard ZnO values, (JCPDS NO. 36-1451) .Furthermore, the ratio between the lattice constants (c/a) was estimated to be 1.60, suggesting all the prepared samples exhibit a hexagonal structure of the ZnO. The value of the practical network constant (a) ranges between 3.26030 and 3.27232 Å, which are values greater than the value of the reference lattice constant is 3.24982 Å. As for the network constant (c), the values of the process range between 5.24080 and 5.22458 Å, w9hich are also greater than the reference (c) value 5.20661 Å, This increase is explained by the presence of an expansion of the lattice resulting from the presence of bromine that occupy interstitial sites within the ZnO crystal. The strain of undoped and doped ZnO, we note that the strain value is maximum when doping 2% with a value of 0.00656, then it decreases sharply at 4% Then the strain increases slightly at 6 %, and reaches its lowest value at 8% with a value of 0.00345 (see table. III.4.)

Table III.4: The Structural parameters of ZnO:Br

Br%	(hkl)	D(nm)	D(moy)	2Θ(°)	a(Å)	c(Å)	c/a	Strain	δ (line/nm^2)
0	(100)	23.43	29.91	31.75	3.2685		1.5988	0.00372	11.1×10^{4}
	(002)	40.45		34.46		5.2260			
	(101)	24.87		36.33					
2	(100)	40.16	32.30	31.70	3.27232		1.6015	0.00656	9.5×10^{4}
	(002)	28.30		34.36		5.24080			
	(101)	28.44		36.21					
4	(100)	40.17	44.92	31.76	3.26630		1.5999	0.00373	4.9×10^{4}
	(002)	47.19		34.46		5.22605			
	(101)	47.42		36.24					
6	(100)	46.86	47.16	31.76	3.26630		1.5986	0.00429	4.4×10^{4}
	(002)	47.19		34.45		5.22899			
	(101)	47.45		36.45					
8	(100)	40.17	42.42	31.83	3.26030		1.6024	0.00345	5.4×10^{4}
	(002)	40.45		34.47		5.22458			
	(101)	47.42		36.24					

.

III.3.3 Optical study

Fig.III.9 shows the optical transmittance of ZnO thin films with various Br doping concentrations using UV–Vis spectrophotometer at wavelength range 300–800 nm. The variations in the thickness influence significantly the optical transmittance which means that the average transmittance of the film increases as Br doping concentrations increases. The increase in transmittance may be attributed to the improvement of crystallinity and surface homogeneity, lowering of defect density and decreasing in scattering of light on the surface. Particularly the films prepared at 6 % Br, which show high optical transmittance [8, 3]. It was also seen that the absorption edge shifted towards a shorter wavelength, i.e., a blue shift, with the increasing of doping concentration. This absorption results from the transition of electrons from the valence band to the conduction band.

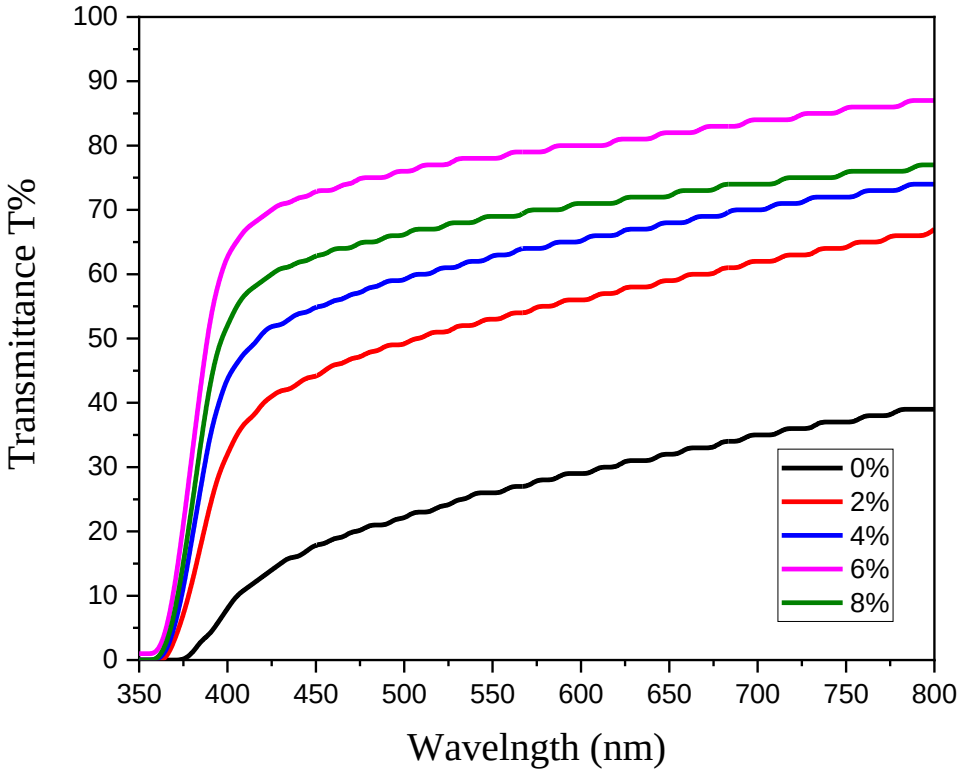

Fig III.9: The transmittance spectra of undoped and Br doped ZnO

III.3.3.1 .Band gap energy:

The band gap of the films can be concluded from a plot $(\alpha h\nu)^2$ vs photon energy ($h\nu$) and extrapolating the straight line portion of this plot to the energy axis (see Fig. III.10.).

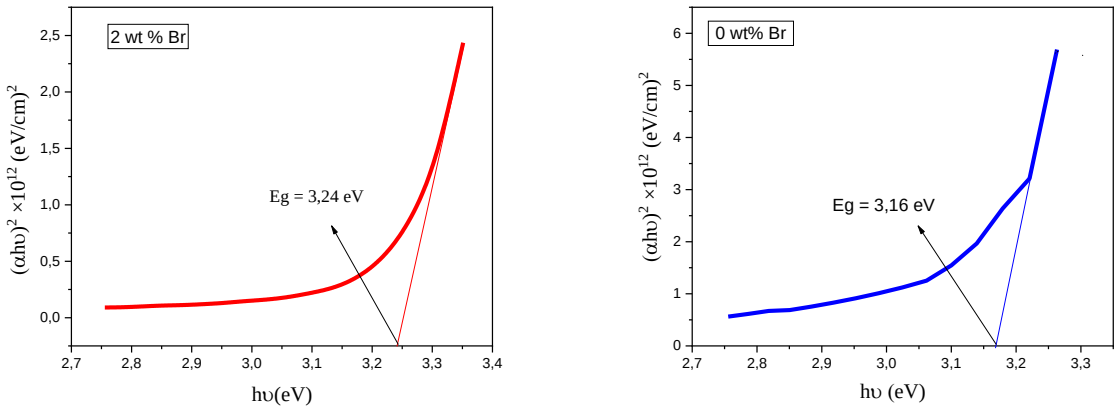

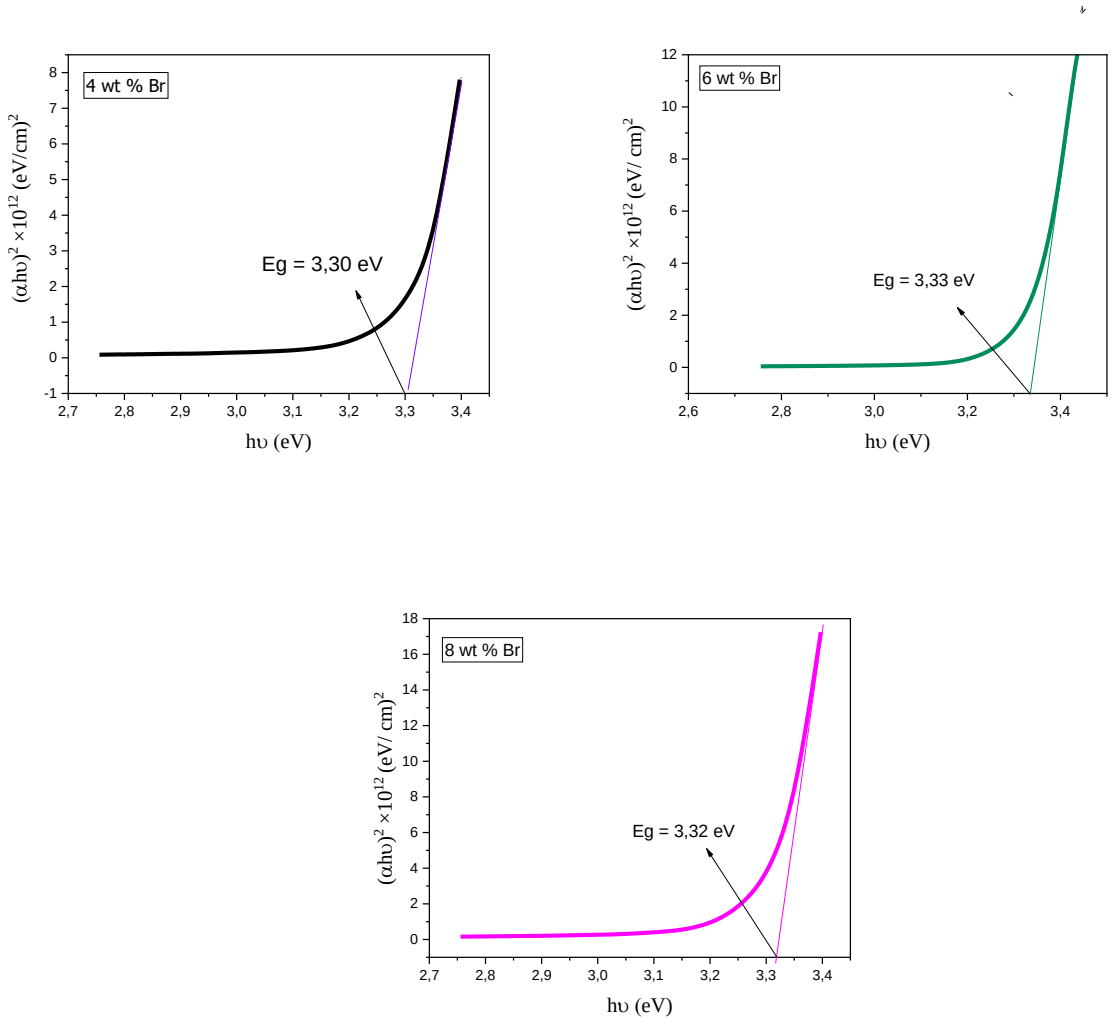

Fig III.10: Plots of $(\alpha h\nu)^2$ versus hυ for the calculate the gap energy

Fig. III.11 shows the variations of band gap as a function of doping concentration. The band gap energy values are in the range of 3,16 - 3,33 eV. It can be observed that Eg increases with the increasing of bromine content. The broadening is attributed to the amelioration of crystalline quality of the films and the reduction of the dislocation. Therefore, there is an agreement with XRD analysis and the achieved results. On the other hand, the band gap widening might be due to the Burstein–Moss effect [8, 9]

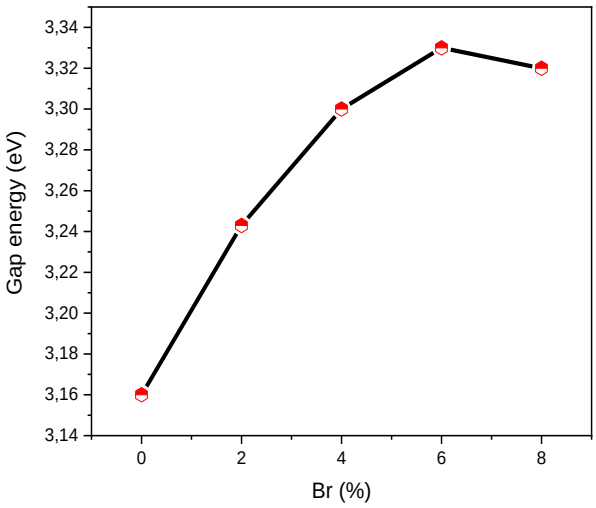

Fig III.11.Variation of band gap with doping concentration Br

III.3.3.2. Urbach energy:

The Urbach tail is an essential parameter used to estimate the level of crystallinity and structural defect or degree of disorder present in the film materials. Generally, the optical transmittance and optical band gap structure affected by the width of localized states available in the films which are known as Urbach tail. This exponential tail appears in the low crystalline, poor crystalline, the disordered and amorphous materials because these materials have localized states which extended in the band gap [5].

Table. III.5 shows the Urbach energy of undoped and Br-doped ZnO films. The Urbach energy values in our ZnO films range between 0.97 eV and 1.62 eV. It is noted that the addition of doping leads to a decrease in the Urbach energy.

Table III.5: Optical band gap the Urbach energy values of undoped and Br doped ZnO

Br (%)	0	2	4	6	8
Eg (ev)	3.17	3.243	3.313	3.341	3.315
Eu (ev)	1.622	1.369	1.48	0.972	1.205

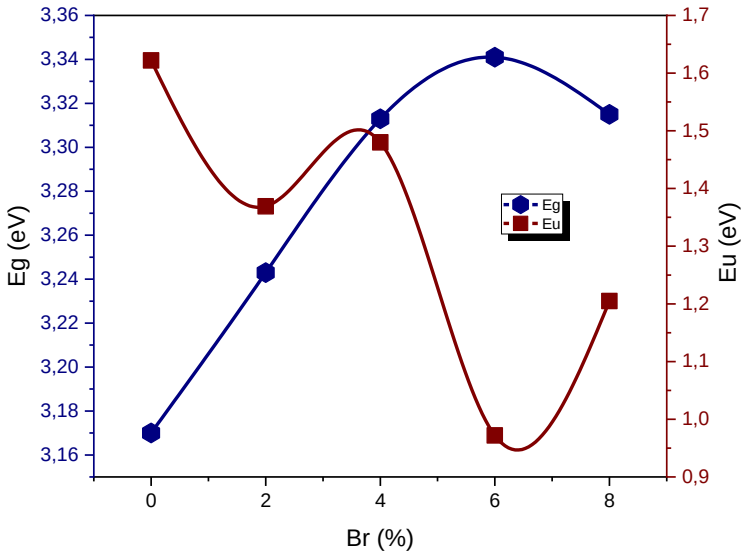

Fig III.12: gap energy and the Urbach energy as functions of Br-doping.

The variation of band gap and Urbach energy as function of doping concentration is shown in Fig.III.12. It can be seen that the band gap is inversely proportional to the Urbach energy (Eu).So, the increase in the band gap might be attributed to the decrease in the band tail width (Urbach tail). It is known that Urbach tail energy depends on point, linear and surface defects. So the disordered materials produce localized states extended in the band gap, which lead to a reduction in the optical band gap energy [10]. However, the decrease in Urbach energy is attributed to the vanishing of localized states and this indicates the improvement in crystallinity of the films (as shown by the XRD patterns) [8] Many studies have found these results [4, 6, 11] .The low Urbach energy also indicates good crystallization of the films.

III.3.4 Electrical study

The measured electrical conductivity of undoped and Br doped zinc oxide thin films is given in Fig III. 13. It can be seen that the conductivity is decreased from 6.8×10^{-3} to 1.6×10^{-3} $(\Omega.\ m)^{-1}$ as increasing Br concentration. We obtained a maximum electrical conductivity value at 6.8×10^{-3} $(\Omega.m)^{-1}$ for undoped ZnO thin film. The reason for the decrease in conductivity is that some Br atoms may occupy interstitial positions and may also form defects in the structural lattice, which acts as a carrier traps rather than electron donors [5]

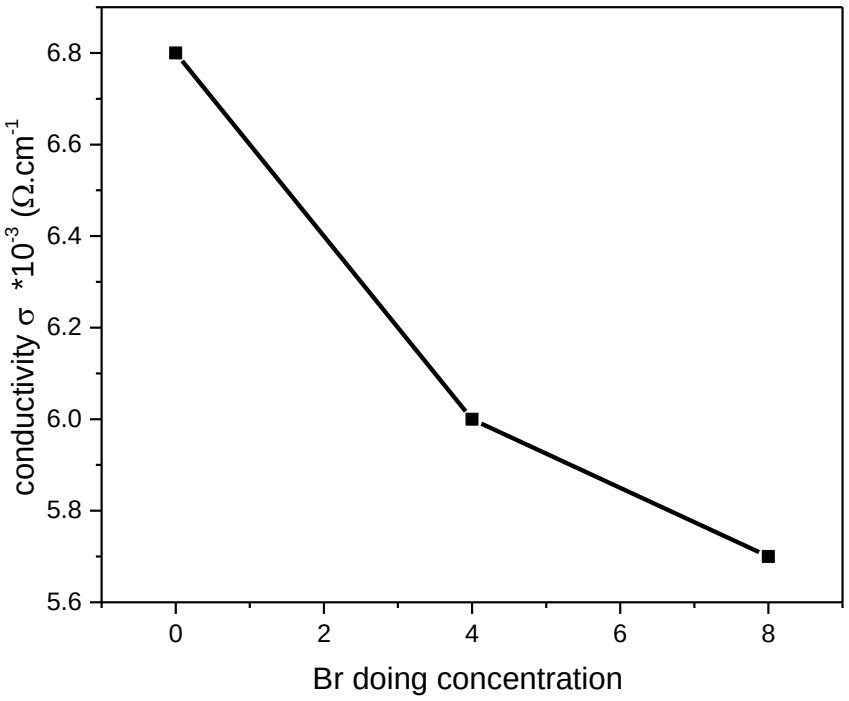

Fig.III.13. Conductivity of prepared Zno thin films.

Table III.6: Electrical values of undoped and Br doped ZnO

Br doping	0	2	4	6	8
Conductivity $(\Omega.\ m)^{-1}$	6.8×10^{-3}	1.6×10^{-3}	6×10^{-3}	1.7×10^{-3}	5.7×10^{-3}

References

[1] Amraoui F, Imane G, The Influence of Calcination Temperature on Properties of Thin films of Zinc-Oxide (ZnO) elaborated by Sol-gel (Dip-coating) Master memory. (2022).

[2] Meethal, B. N., & Swaminathan, S. Bromine-induced defects in anion-deficient zinc oxide as stable photocatalysis promoters. ChemistrySelect, 3(47), 13345-13354. (2018).

[3] Rafique, S., Kasi, A. K., Kasi, J. K., Bokhari, M., & Shakoor, Z. Fabrication of Br doped ZnO nanosheets piezoelectric nanogenerator for pressure and position sensing applications. Current Applied Physics, 21, 72-79. (2021).

[4] Benramache, S., Benhaoua, B., & Belahssen, O. The crystalline structure, conductivity and optical properties of Co-doped ZnO thin films. Optik, 125(19), 5864-5868. (2014).

[5] Yahia, A. Optimization of indium oxide thin films properties prepared by sol gel spin coating process for optoelectronic applications (PhD Thesis, University Mohamed Khider Biskra). (2020).

[6] Kherchachi, I. B., Attaf, A., Saidi, H., Bouhdjar, A., Bendjdidi, H., Youcef, B., & Azizi, R. The synthesis, characterization and phase stability of tin sulfides (SnS 2, SnS and Sn 2S 3) films deposited by ultrasonic spray. Main Group Chemistry, 15(3), 231-242. (2016).

[7] Prathap, P., Devi, G. G., Subbaiah, Y. V., Reddy, K. R., & Ganesan, V Growth and characterization of indium oxide films. Current Applied Physics, 8(2), 120-127. (2008).

[8] Bennaceur, K. Elaboration and characterization of SnO2: In thin films deposited by spray pyrolysis technique (PhD Thesis University Mohamed Khider Biskra). (2020).

[9] Hamani, N. Elaboration et caractérisation des couches minces d'oxyde d'indium dopées à l'étain et au brome obtenue par spray pyrolyse ultrasonique (PhD Thesis, Université de mohamed kheider biskra). (2021).

[10] L'effet de l'amplitude d'onde ultrasonique sur les propriétés optiques et électriques des couches minces de ZnO déposé s par spray ultrasonique (PhD Thesis, Université Mohamed Khider of Biskra).(2012).

[11] Dahnoun, M. Preparation and characterizationof Titanium dioxide and Zinc oxide thin films via Sol-Gel (spin coating) technique for optoelectronicapplications (PhD Thesis, University Mohamed Khider of Biskra). (2020).

General conclusion

In this study we have deposited and characterized thin films of undoped and doped zinc oxide using pneumatic spray technique on glass substrates. The effect of different concentration of bromine doping on the structural, optical and electrical properties had been investigated to give good quality films.

The structural properties of the deposited films have been analyzed using X-ray diffraction (XRD) while the optical properties are investigated by UV-VIS spectroscopy, and the electrical properties have been obtained by four probes method.

The film thickness, measured by gravimetric method, ranged from 285 to 570 nm. X-ray diffraction study showes that all the films prepared have polycrystalline hexagonal wurtzite phase structure with (100), (002) and (101) preferential orientation. The average crystallite size of the ZnO films was observed as approximately 47.16 nm in the film doping with 6 wt% ZnO:Br concentration.

The UV-Visible study shows that values of transmittance is high in the visible region and minimum at wavelength in the absorbance edge (300-400 nm), it's ranging from 40 to highest value 80% at 6 wt% Br. The shift of optical transmittance toward a shorter wavelength can be shown by the increase of bandgap energy from 3.16 eV to 3.33 eV with increasing of doping concentration. The observed Urbach energy of ZnO: Br thin films decreases from 1.622 eV to 0.972 eV.

The electrical conductivity reveals a decrease on its value as the bromine doping increase, whereas it has the highest value 6×10^{-3} $(\Omega.m)^{-1}$ at 4 wt% of bromine concentration.

Finally, we can say that doping enhance the optical properties specially the transmittance of the films, which make them very suitable for photovoltaic applications, while we must ameliorate the electrical properties specially the conductivity of the films in order to use them in gas sensor applications.

The effect of bromine doping rate on the properties of ZnO thin films

Abstract

In this work, we deposited thin films of unpoped and doped zinc oxide (ZnO) with bromine (Br) in different proportions (2%, 4%, 6%, 8%) on glass substrates by pneumatic spray pyrolysis. The characterization of the films was studied by X ray diffraction (XRD), visible UV spectroscopy and the four point method .the results XRD showed that all samples have a compact hexagonal structure of polycrystalline zinc oxide, with a preferential growth direction (002). In our work, we found that crystalite size increase in the ranges from 29.91 to 47.16 nm. The optical study showed that the transmittance increases with increasing the doping percentage, and its highest value was at the doping percentage of 6%, reaching 85%, In addition, The energy gap was also calculated, and we found that it increases with increasing doping percentage, ranging from 3.17 to 3.34ev, while the Urbach energy decreases with increasing doping. Electrical measurements indicated All films have a conductivity in the range from 1.6×10^{-3} to 6.8×10^{-3} $(\Omega.\ m)^{-1}$.

Keywords: Thin films, ZnO, TCO, Pneumatic spray, DRX, Br , doping, Optical and electrical properties

تأثير نسبة التطعيم بالبروم على خواص الشريحة الرقيقة ZnO

ملخص

في هذا العمل ، قمنا بترسيب أغشية رقيقة من أكسيد الزنك (ZnO) الغير مطعم والمطعم بالبروم (Br) بنسب مختلفة (2٪ ، 4٪ ، 6٪ ، 8٪) على ركائز زجاجية بتقنية الرش بمرذاذ الهواء المضغوط . لتوصيف الشرائح استعملنا انعراج الأشعة السينية، مطيافية الأشعة فوق البنفسجية و تقنية أربع مسابير. تمت دراسة الخواص البنيوية والبصرية و الالكترونية لهذه الاغشية .نتائج فحوصات الاشعة السينية (DRX) بينت أن جميع العينات تظهر بنية سداسية متراصة متعددة البلورات لاكسيد الزنك, و باتجاه نمو المفضل (002) للطبقات ، وجدنا ايضا زيادة في الحجم الحبيبات حيث يتراوح بين 29.91 و 47.16 نانومتر. فيما يخص نتائج تحليل الأشعة فوق البنفسجية اظهرت ان النفاذية للشرائح تزداد مع زيادة نسبة التطعيم حيث بلغت اكبر قيمة للنفاذية حوالي (87%) في المجال المرئي للضوء عند 6٪ ، بالاضافة إلى ذلك اظهرت النتائج ان فجوة الطاقة الضوئية تزداد بزيادة التطعيم حيث تتراوح بين 3.17 الى 3.34 الكترون فولط , بينما تتناقص طاقة اورباخ. القياسات الكهربائية اظهرت ان كل الافلام تملك ناقلية . تتراوح من 1.6×10^{-3} إلى 6.8×10^{-3} $(\Omega.$ متر$)^{-1}$.

الكلمات المفتاحية : الاغشية الرقيقة , ZnO , TCO, تقنية الرش بالهواء المضغوط، DRX , Br , التطعيم , خصائص ضوئية وكهربائية